

University of Montana

ScholarWorks at University of Montana

Graduate Student Theses, Dissertations, &
Professional Papers

Graduate School

2005

K-bentonites of the Middle Proterozoic Belt Supergroup western Montana

Michelle L. Foster

The University of Montana

Follow this and additional works at: <https://scholarworks.umt.edu/etd>

Let us know how access to this document benefits you.

Recommended Citation

Foster, Michelle L., "K-bentonites of the Middle Proterozoic Belt Supergroup western Montana" (2005).
Graduate Student Theses, Dissertations, & Professional Papers. 7550.
<https://scholarworks.umt.edu/etd/7550>

This Thesis is brought to you for free and open access by the Graduate School at ScholarWorks at University of Montana. It has been accepted for inclusion in Graduate Student Theses, Dissertations, & Professional Papers by an authorized administrator of ScholarWorks at University of Montana. For more information, please contact scholarworks@mso.umt.edu.



Maureen and Mike
MANSFIELD LIBRARY

The University of
Montana

Permission is granted by the author to reproduce this material in its entirety, provided that this material is used for scholarly purposes and is properly cited in published works and reports.

****Please check "Yes" or "No" and provide signature****

Yes, I grant permission

X

No, I do not grant permission

Author's Signature: _____

Michael L. L. F.

Date: _____

12/23/05

Any copying for commercial purposes or financial gain may be undertaken only with the author's explicit consent.

K-Bentonites of the Middle Proterozoic Belt Supergroup, Western Montana

by

Michelle L Foster

B.S. Georgia State University, 2001

A thesis submitted in partial fulfillment of the

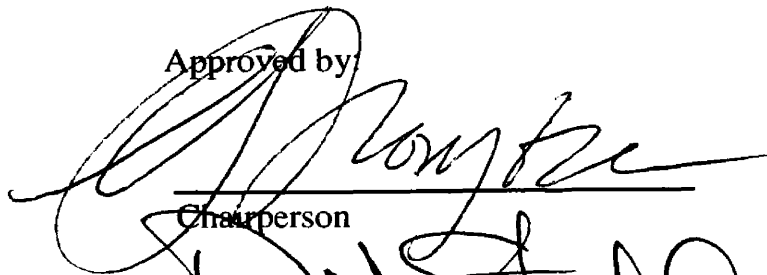
requirements for the degree of

Master of Science


The University of Montana

2005

Approved by

A large, stylized handwritten signature in black ink, written over a horizontal line. The signature is cursive and appears to read "M. L. Foster".

Chairperson

A large, stylized handwritten signature in black ink, written over a horizontal line. The signature is cursive and appears to read "D. J. Steele".
Dean, Graduate School

12-28-05

Date

UMI Number: EP38351

All rights reserved

INFORMATION TO ALL USERS

The quality of this reproduction is dependent upon the quality of the copy submitted.

In the unlikely event that the author did not send a complete manuscript and there are missing pages, these will be noted. Also, if material had to be removed, a note will indicate the deletion.



UMI EP38351

Published by ProQuest LLC (2013). Copyright in the Dissertation held by the Author.

Microform Edition © ProQuest LLC.

All rights reserved. This work is protected against unauthorized copying under Title 17, United States Code



ProQuest LLC.
789 East Eisenhower Parkway
P.O. Box 1346
Ann Arbor, MI 48106 - 1346

K-Bentonites of the Middle Proterozoic Belt Supergroup, Western Montana

Chairperson: Gray Thompson



Numerous previously unrecognized K-bentonites in the Middle Proterozoic Belt Supergroup of western Montana may provide a Rosetta Stone for precise temporal correlation of those rocks with coeval stratigraphic units deposited in intracratonic basins now located in western North America, Siberia, and Australia that may have been tectonically connected during the Middle Proterozoic. Fine-grained siliciclastic and carbonate rocks of the Belt Supergroup cover much of western Montana and parts of Idaho, Washington, and British Columbia, and attain a thickness of more than 18 kilometers at the basin depocenter. Paleogeographic reconstruction places the Belt basin in the center of a supercontinent consisting of Laurentia, Siberia and Australia, where the basin formed in response to incipient rifting. Thus, Belt-equivalent rocks are thought to exist in Siberia and perhaps Australia. Stratigraphic correlation has been difficult, both within the Belt Supergroup and among those modern continents, because of the lack of useful fossils in the ancient rocks. Previous research shows that K-bentonites have geochemical signatures that allow a single K-bentonite to be correlated over great distance, and that K-bentonites contain magmatic minerals useful for precise radiometric dating. In the present study, 32 previously unrecognized K-bentonites have been identified in the Belt Supergroup based on field characteristics, quantitative mineral analyses, illite polytype determinations, chemical analyses, TGA, and SEM imaging. Dissimilarities in outcrop appearance compared to familiar younger K-bentonites may be responsible for previous lack of recognition of Belt K-bentonites, despite more than 100 years of intensive study of Belt rocks.

Table of Contents

Abstract	ii
Table of Contents	iii
List of Figures	v
List of Tables	viii
Acknowledgements	ix
CHAPTER	Page
1. INTRODUCTION	1
Bentonite and K-bentonite	2
The Belt Supergroup	6
2. SAMPLING METHODS	9
Field Identification	9
Sampling Locations	11
3. ANALYTICAL METHODS	13
Qualitative X-ray Diffraction Mineral Analysis	13
Petrography	14
Quantitative X-ray Diffraction Mineral Analysis	14
Semi-Quantitative Interpretations of Qualitative Mineral Analysis	15
Chemical Analysis	17
Thermogravimetric Analysis	17
Scanning Electron Microscopy	17

4. RESULTS	18
Field Characteristics	18
Petrography	23
X-Ray Diffraction Analyses	38
Chemical Analysis	43
Thermogravimetric Analysis	48
Scanning-Electron Microscopy	48
U-Pb Dating	48
5. DISCUSSION	55
Recognition and Identification of Belt K-bentonites	55
Petrographic Data	57
Mineral Compositions	58
Illite Polytypes	60
Chemical Analyses	62
Scanning-Electron Microscopy	64
Source of Illite and K-bentonites in the Belt Supergroup	64
Source of Volcanic Ash in the Belt Basin	64
6. CONCLUSIONS	68
APPENDIX A: X-Ray Diffraction Patterns	LXIX
WORKS CITED	LXXXII

List of Figures

Figure		Page
1	Outcrop appearance of Cretaceous bentonites from the Colorado Group.	10
2	Sample Locations.	12
3	Calibration Curve - Semi-Quantitative Interpretations of Qualitative Mineral Analysis.	16
4a&b	Outcrop Appearance of Recessive Chalky K-Bentonites with Asymmetric Crenulation Cleavage.	19
5	Outcrop Appearance of Recessive Chalky K-bentonites without Asymmetric Crenulation Cleavage.	20
6	K-bentonite Containing Contorted Siltstones Ripped From the Surrounding Beds.	21
7	Outcrop Appearance of Cherty Textured K-Bentonites.	22
8	Photomicrograph of K-Bentonite from the Garnet Range Formation (Missoula Group).	25
9	Photomicrograph of a K-Bentonite from the Garnet Range Formation (Missoula Group).	26
10	Photomicrograph of a K-Bentonite from the McNamara Formation (Missoula Group).	27
11	Photomicrograph of a K-Bentonite from the McNamara Formation (Missoula Group).	28
12a & b	Photomicrograph of a K-Bentonite from the McNamara Formation (Missoula Group).	29
13	Photomicrograph of a K-Bentonite from the McNamara Formation (Missoula Group).	31
14	Photomicrograph of a K-Bentonite from the upper Bonner Formation (Missoula Group).	32

15	Photomicrograph of a K-Bentonite from the Siyeh Limestone (Piegan Group).	33
16	Photomicrograph of a K-Bentonite from the Revett Formation (Ravalli Group).	35
17a&b	Photomicrograph of a Neo-Proterozoic K-Bentonite from the Nama Supergroup, Namibia.	36
18a&b	Photomicrograph of a Ordovician K-Bentonite from the Appalachian Basin.	37
19	Photomicrograph of a Transitional Bed from the Revett Formation (Ravalli Group).	39
20	Photomicrograph of a Detrital Bed from the Revett Formation (Ravalli Group).	40
21	X-Ray Diffraction Multi-plot of a K-Bentonite from the Revett Formation (Ravalli Group) Comparing Heat Treated and Glycol Solvated Patterns.	44
22	X-Ray Diffraction Multi-plot of a K-Bentonite from the Wallace Formation (Piegan Group) Comparing Heat Treated and Glycol Solvated Patterns.	45
23	X-Ray Diffraction Multi-Plot Showing Sample Heterogeneity.	46
24	Thermogravimetric Analysis Plot of a K-Bentonite from the Garnet Range Formation (Missoula Group).	49
25	Thermogravimetric Analysis Plot of a K-Bentonite from the Upper Bonner Formation (Missoula Group).	50
26	Thermogravimetric Analysis Plot of a K-Bentonite from the Revett Formation (Ravalli Group).	51
27	Scanning Electron Microscope Photo of a K-Bentonite.	52
28	Scanning Electron Microscope Photo of a K-Bentonite Showing Euhedral Calcite Grain.	53

29	Total Clay vs. Quartz Content of Belt K-Bentonites Plotted Against Belt Sedimentary Rocks and Paleozoic Shales.	59
30	Plot of % 1M Illite vs. % 2M ₁ Illite of Belt K-Bentonites.	61
31	Magma Discrimination Diagram Nb/Y vs Zr/TiO ₂ .	63
32	Proposed Southeastern Source Region for Illite, Chlorite, and K-Bentonites in the Belt Supergroup (Sears, in review).	66

List of Tables

Table		Page
1	Stratigraphic and Geologic Locations and X-Ray Diffraction Mineral Analysis Results	41 & 42
2	Chemical Analysis Results	47

Acknowledgments

I would like to thank Dr Gray Thompson for his patience and knowledge; Dr Don Winston and Dr Jim Sears for pointing me to possible K-bentonites in the Belt; Dr Warren Huff, Dr Pete Ryan, and Dr Beverly Seylor for lending me thin sections of known K-bentonites, I would also like to thank Dr Huff for his insight into bentonites and K-bentonites; Dr Dougal McCarty and his staff at Chevron-Texaco and Dr Kevin Chamberlain for assistance with the data I collected; Dr Steve Sheriff, Loreene Skeeel, and Christine Foster for some department funding; The Clay Minerals Society for grant support that made this project possible; Aron Langley for carrying rocks; and my friends (you know who you are) and family for their support.

CHAPTER 1

INTRODUCTION

Many scientists who study the middle Proterozoic Belt Supergroup infer that it was deposited in an intracratonic rift environment (eg: Winston, 1986, Frost and Winston, 1987, Ross and Villeneuve, 2003, Sears, in review). Intracratonic rift environments are commonly accompanied by a bimodal suite of mafic and felsic rocks (Hyndman, 1985, Christiansen and Lipman, 1972, Moyer and Nealey, 1989, Pallister, 1987) yet evidence of felsic volcanism is strikingly absent from literature describing the Belt Supergroup (Link et al., 2003, Winston, 1986). The only published evidence of felsic volcanism prior to this study is the Purcell Lava in southeastern British Columbia and northwestern Montana, a basalt flow that contains about 6 meters of a 'regionally unique' rhyolite or quartz latite flow (Johns, 1961 in Evans et al., 2000), and two K-bentonites, one in the upper Wallace Formation of the Pigeon Group in Glacier National Park (Goldich et al., 1959, Moe et al., 1996) and the other at the contact between the Libby Formation and the Bonner Formation just west of Libby, Montana (Kidder, 1992, Evans et al., 2001).

I propose that felsic volcanism was common during deposition of the middle Proterozoic Belt Supergroup of western Montana and supplied considerable quantities of sedimentary material including bentonites to the Belt Basin, but that bentonites deposited by this process have gone largely unrecognized by previous workers. I also suggest that

felsic volcanism was the source of the large volume of clay minerals (now illite and lesser amounts of chlorite) present in the Belt Supergroup.

Goldich et al, 1959, and Moe et al, 1996, described a 20 centimeter-thick olive-green K-bentonite bed in the uppermost Piegan Group in a road cut at Logan Pass in Glacier National Park. Kidder (1992) and Evans et al. (2001) described one additional K-bentonite bed occurring near the contact between the Bonner Formation and the Libby formation, just west of Libby, Montana. These are the only bentonites that have been described from the Belt Supergroup prior to this paper.

The major goal of the research described in this paper is to identify and characterize K-bentonites throughout the Belt Supergroup, to determine their abundance and distribution, to evaluate their mineralogical and chemical characteristics, and to assess the importance of volcanogenic contributions to the Belt Supergroup.

Future analyses of these previously unrecognized and abundant volcanic beds in the Belt Supergroup may establish time synchronous marker beds for correlations with age equivalent strata throughout North America and with strata now located on other continents. Data obtained from these bentonites may also provide accurate time constraints for Belt sedimentation rates.

Bentonite and K-Bentonite

Bentonites are clay rich relics of volcanic ash deposited in aqueous environments and are commonly interbedded in shale, sandstone, and carbonate rocks (Dennison and Textoris, 1970 in Altaner et al., 1984; Weaver, 1956; Hoffman, 1976; Hoffman and Hower, 1979; Weaver et al., 1980). Bentonites have a higher preservation

potential in shale and fine-grained carbonate rock as a result of the low current velocities associated with such facies. Stratigraphic continuity, uniform groundmass, presence of quartz shards, euhedral zircon and other magmatic crystals, and clay mineral composition provide evidence that bentonites originate from air fall ash (Moe, et al., 1996; Kolata, et al., 1996; Grim, 1978). Most have a waxy, soapy or chalky appearance, range in color from greenish gray/blue to light grey or tan, and vary in thickness from several millimeters to several meters (Kolata et al., 1996).

Bentonites commonly occur as recessive layers having sharp lithologic contact with the underlying strata and a sharp or gradational contact with the overlying strata. Renewed detrital input, combined with terrigenous volcanic ash, may result in a transitional layer immediately above the bentonite (Hayes, 1994, Huff, personal communication, 2004). Slaughter and Earley (1956) described Upper Cretaceous Mowry bentonites in north-central Wyoming as having two outcrop appearances. Some of these bentonite beds have a sharp contact with bounding porcelanite beds, while other bentonite beds have a gradational contact with the overlying shale bed.

“Mixed” bentonites form from volcanic ash that has been reworked by physical processes such as waves, tides, and currents and “secondary” bentonites form from volcanic ash that has been eroded, transported, and re-deposited by flowing water (Huff, personal communication, 2005; Ver Straeten, 2004). Mixed bentonites and secondary bentonites may exhibit sedimentary structures that reflect their depositional histories, and may be easily overlooked.

In marine environments, volcanic ash reacts with seawater resulting in a loss of silica, potassium, and calcium, and a gain in sodium, water, and magnesium;

subsequently crystallizing as minerals of the smectite group (Grim and Guven, 1979, Kiersch and Keller, 1955, Altaner, 1985, Walker, 1983). The excess silica in the system may accumulate as secondary silica in the overlying beds (Rosenkrans, 1936,) and underlying beds (Slaughter and Earley, 1965, in Altaner, 1985) and may re-crystallize as cristobalite (Gruner, 1940) or quartz in the bentonite. Chertification of the underlying or overlying strata may develop if the host rock is a carbonate.

Under low-grade metamorphic conditions of at least 100°C, (or lower temperatures at longer periods of time (Ryan, 1991), and with a source of potassium, the potassium-poor smectite alters to potassium-rich illite as the bentonite converts to K-bentonite (Altaner, 1985; Walker, 1983). Thus, K-bentonites differ from bentonites in that they contain illite or mixed-layered illite-smectite (I/S) instead of smectite as the dominant mineral (Altaner et al. 1984; Hoffman, 1976, Walker, 1983). The potassium content of the K-bentonite is proportional to the percentage of illite layers in the I/S clay (Hoffman, 1976). Most Paleozoic K-bentonites contain approximately 60% to 90% illite layers (Altaner, 1985, Moe et al, 1996). The two previously described Precambrian K-bentonites in the Belt Supergroup, Montana, contain 100% illite layers (this study). Proposed environments of illitization of smectite and conversion of bentonite to K-bentonite include burial metamorphism (Weaver and Wampler, 1970, Perry and Hower, 1972, and Hower et al., 1976) and metasomatism (Velde and Brusewitz, 1982, Elliott et al., 1987, McCarty, 1990). The Cretaceous K-bentonites in the disturbed belt in northwestern Montana (Altaner et al., 1984, Hoffman and Hower, 1979), like many other K-bentonites, have carbonates and shales as host rock.

Illite polytypes indicate the diagenetic and detrital history of clay rich rocks (Eslinger and Sellars, 1981, Ryan, 1991; Walker and Thompson, 1990). 1M is the low temperature polytype of illite, and is concentrated in the clay size fraction (Srodon and Eberl, 1984). With increasing metamorphic grade, 1M transforms to the higher temperature 2M₁ polytype, resetting the K-Ar clock. K-Ar dating of the 2M₁ polytype thus yields a younger diagenetic age, thereby distinguishing it from older detrital 2M₁ illite (Srodon and Eberl, 1984).

Some K-bentonite beds are mineralogically zoned, characterized by high K₂O content and percent I in I/S near the bentonite margins with decreasing values toward the center of the bentonite bed. This stratified characteristic is the result of slow diffusion of K₂O into the bentonite during the illitization process (Altaner et al., 1984, Walker, 1983, Velde and Brusewitz, 1982). It has been shown that mineralogic zonation may occur in response to different permeability of the underlying and overlying bounding sedimentary layers (Velde and Brusewitz, 1982, Brusewitz, 1986) and proximity to heat sources (Altaner et al., 1984, Ryan, 1996) such as a dike or sill.

A violent volcanic eruption commonly deposits a wide-ranging, time synchronous blanket of volcanic ash containing angular and euhedral quartz, zircon, feldspar, apatite and other magmatic crystals, which are incorporated in the air fall ash as it accumulates on the earth's surface. These ash layers may be directly preserved in the sedimentary sequence eventually to become bentonites and K-bentonites, they may be reworked after initial deposition by currents, tides, or waves to become "mixed" bentonites and K-bentonites, or they may be eroded, transported, and eventually re-deposited to form "secondary" bentonites or K-bentonites. If dilution by non-

volcanogenic sediments is relatively minor, the resulting deposit can retain many of the characteristics of a bentonite formed directly from an air-fall ash. However, this dilution may mix detritally rounded grains of quartz, feldspar, mica, zircon and other minerals with the ash component. Zircon grains are extremely resistant to weathering and are commonly used for uranium-lead and lead-lead radiometric dating and stratigraphic correlation (Schirnack, 1990, Ray et al., 2002). However, if older detrital zircons are not separated from zircons formed during the most recent volcanic event, the zircon ages will represent a weighted average of the zircons from the various crystallization times. Thus, SHRIMP methods have proved most useful in dating many bentonites and K-bentonites (Evans et al., 2000).

Individual K-bentonites have distinct chemical signatures. Bergstrom et al. (1995) and Kolata et al. (1996) used chemical signatures of Ordovician K-bentonites to correlate them within the Appalachian Basin, as well as to correlate K-bentonite beds of the Appalachian Basin to K-bentonite beds in Baltoscandia. Huff et al. (1997) applied similar techniques to a Silurian K-bentonite of the Appalachian Basin, and Seylor et al. (in review) used similar methods to correlate K-bentonites in the late Proterozoic African Nama Group. Chemical analysis of Belt bentonites may provide a similar tool for basin-wide and inter continental correlations in the Belt Supergroup and correlative units in North America and on other continents.

The Belt Supergroup

The Middle Proterozoic Belt Supergroup is a thick, extensive sedimentary sequence that underwent several episodes of faulting and folding following deposition. It is

greater than 18 km thick at its depocenter, and spans western Montana, northern and central Idaho, eastern Washington, British Columbia, and Alberta. Although the Belt Supergroup has been considered an open marine deposit (Harrison, 1972), recent investigations favor an enclosed intracratonic rift basin (Winston et al., 1986, Frost and Winston, 1987, Ross and Villeneuve, 2003, Sears, 2005, in review).

The Belt Supergroup is separated into four Groups: 1) the lower Belt, the Ravalli Group, the Piegan Group (to be resurrected), and the Missoula Group (Winston, personal communication 2003). Original lithologies include coarse to fine-grained arenite and silt, red and green mudstone, argillaceous carbonate, and dark gray laminated argillite and sandstone (Winston, 1986).

The presence of voluminous mafic sills, occasional lava flows, and the K-bentonites discovered in this study in the Belt Supergroup support the interpretation of an intracontinental rift environment, and also suggest the importance of magmatic activity during deposition of those sediments (Zartman et al. 1982; Burwash and Wagner, 1989; Evans and Fischer, 1986). The large amounts of illite and chlorite in the Belt basin (Ryan, 1991) may have formed from the weathering of felsic volcanic materials. Schieber (1993) suggested that weathering of volcanic rocks may be the source for the “discrepancies between the likely K content of the hinterland and the actual K content of Belt sediment”. Eslinger and Sellars (1981) also suggested a volcanic contribution to the Belt sediments, concluding that the ‘enigmatically’ large amount of illite in the Belt Supergroup may be of volcanic origin, and Bleiwas (1977) suggested a volcanic source for the chert beds in the upper McNamara Formation. In addition, the Southern Granite-

Rhyolite Province active during Belt time and may have been the source of K-bentonites in the Belt Supergroup (Sears, in review 2005).

The Belt-Purcell rift system initiated at about 1510-1485 Ma (Lydon, 2000). Diabase dikes (Zartman et al. 1982; Burwash and Wagner, 1989), the Purcell lava (Evans et al., 2000) and the Alderson Lake sill (R.A. Burwash, personal comm., in Moe et al., 1996) were emplaced within the basin at 1430-1450 Ma and 1307 Ma, respectively. The Windermere group represents the first rifting sequence during latest Neoproterozoic at about 740 Ma to 723 Ma (Ross et al., 1995 in Colpron et al., 2002). A second Neoproterozoic age of 569 Ma was established by U-Pb dating of zircons from synrift volcanic rocks of the Hamill Group in the southeastern Cordillera indicating a latest rifting age for the Belt basin (Colpron et al., 2002).

CHAPTER 2

SAMPLING METHODS

Field identification

I initially explored for bentonites in the Belt Supergroup by looking for sedimentary beds showing field characteristics similar to those of known, well-described, younger bentonites. Figure 1 illustrates characteristic outcrop appearances of Cretaceous bentonites in the Colorado Group along the Missouri River between Carters Ferry and Ft. Benton, Montana. Typical bentonites are regionally extensive, recessive in outcrop and range in thickness from several millimeters to several meters. They are white to light grey or tan, chalky, clay-rich and have a waxy texture when wet (Haynes, 1994, Kolata et al. 1996, Ross, 1928). Bentonites may not exhibit sedimentary structures if they are primary air fall ash beds, but may exhibit sedimentary structures if they have been reworked to form “mixed” bentonites, or “secondary” bentonites if they were initially deposited by flowing water (Huff, personal communication, 2004).

I soon discovered, however, that perhaps because of their great age, many Belt bentonites do not closely resemble typical younger bentonites described by previous workers. Thus, we began developing criteria for recognizing these ancient clay-rich beds in the field. These criteria are described at the beginning of Chapter 5. To date, I have identified and analyzed 32 K-bentonites, “mixed” K-bentonites, and “secondary” K-



Figure 1: Cretaceous bentonites, from the Colorado Group located between Carters Ferry and Fort Benton along the Missouri River, are recessive clay rich beds.

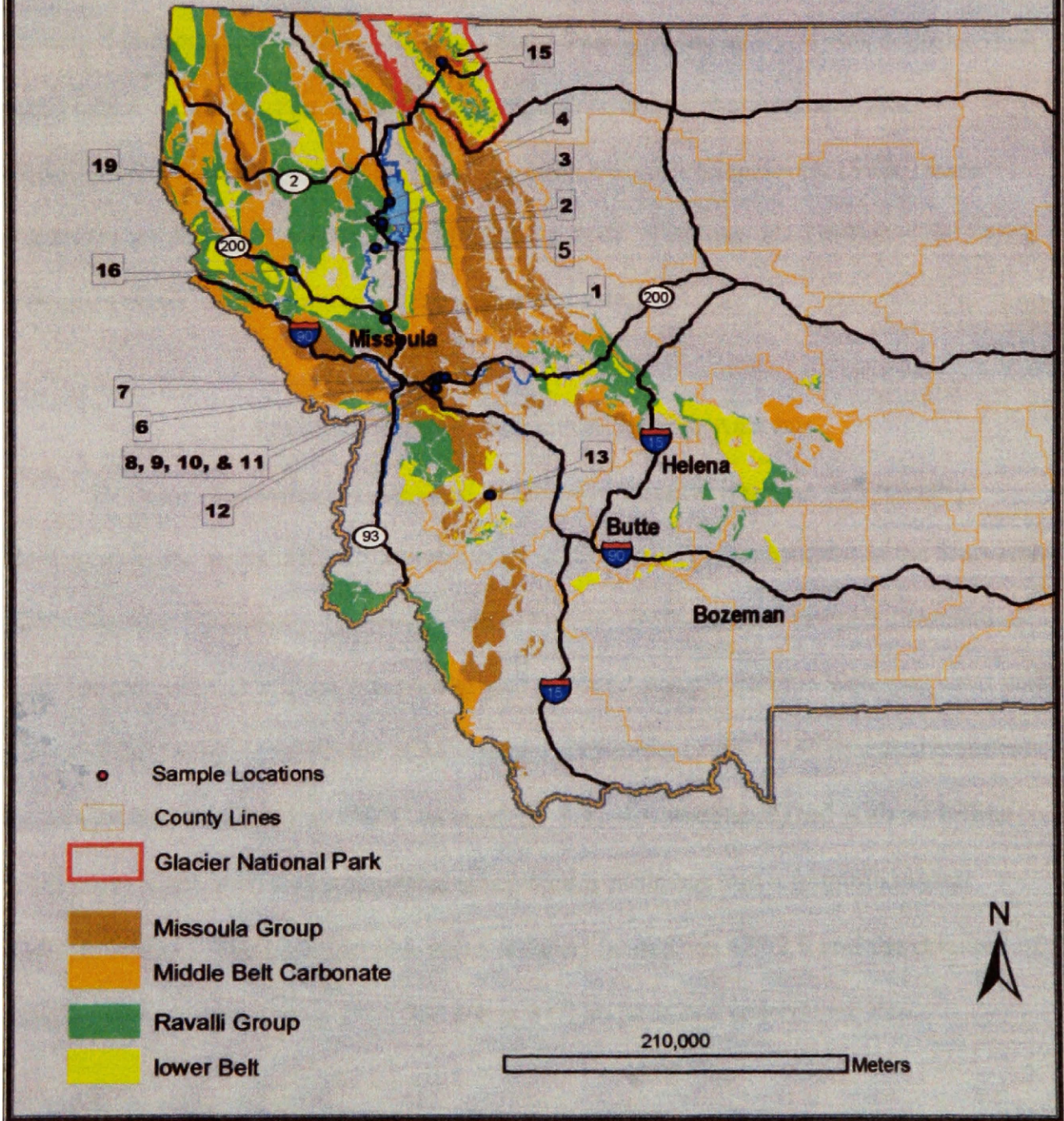


bentonites ranging in thickness from 5 cm to 35 centimeters, from 19 different localities and 9 formations in Belt rocks from western Montana

Sampling locations

Belt K-bentonites and the bounding siltstones, sandstones, and argillites were collected from the Ravalli Group, the Piegan Group and the Missoula Group for preliminary investigation (Figure 2). All sample locations are described in Table 1 on Pages 41 and 42. Samples of the K- bentonites and the bounding beds were collected for further study by the following analytical methods.

Figure 2: Location Map of K-bentonites in the middle Proterozoic Belt Supergroup, western Montana



CHAPTER 3

ANALYTICAL METHODS

Qualitative x-ray diffraction (XRD) analysis was conducted on all tentatively-identified K-bentonites and the bounding beds. Petrographic analysis was conducted on many of the same samples. Quantitative mineral analysis, chemical analysis, thermogravimetric analysis (TGA), and scanning electron microscopy (SEM) were conducted on selected bentonites and bounding beds. Uranium-lead radiometric dating was also conducted on zircons from one K-bentonite.

Qualitative X-ray Diffraction Mineral Analysis

Because bentonites are clay-rich, qualitative mineral analysis was initially conducted in the x-ray diffraction laboratory at the Geology Department at the University of Montana on all samples to estimate clay content. Bulk random samples prepared in back-loaders and < 2 micron oriented glycol solvated sample mounts were prepared and analyzed following the methods of Moore and Reynolds, (1997). 001 oriented samples were heated for one hour at 550°C as needed. Samples were analyzed with a Phillips XRG 3100 X-ray diffraction machine using CuK α radiation and a graphite crystal monochromator. The bulk samples were scanned from 5° to 65° 2 θ and the oriented samples were scanned from 2° to 70° 2 θ at 0.02 steps at one second per step.

Petrography

Thin sections were examined to identify features indicative of volcanic origin including euhedral and angular crystals and shards, β quartz relics, “floating” grains (clay matrix-supported coarser grains), and fluid inclusions (Blatt, 1980; Moe, et al., 1996; Kolata, et al., 1996; Grim, 1978); and to identify textures indicative of detrital transport, including rounded grains and grain-supported textures. The K-bentonites were cut perpendicular to bedding for thin section preparation when possible. Thin sections were also examined for many detrital units bounding the K-bentonite layers.

Don Winston of the Geology Department at the University of Montana loaned two-dozen thin sections of siltstones and sandstones from the Belt Supergroup. Peter Ryan, from the Geology Department at Middlebury College, donated four thin sections from suspect bentonites in the Ravalli Group along highway 93. Warren Huff of the Geology Department at the University of Cincinnati loaned a dozen thin sections from his collection of Ordovician K-bentonites from the Appalachian Basin (Huff et al., 1997), and Beverly Seylor of the Geology Department at Massachusetts Institute of Technology loaned more than a dozen thin sections of K-bentonites from the Neo-Proterozoic Nama Group in southwestern Namibia (Seylor et al., in review).

Quantitative X-ray Diffraction Mineral Analysis

Quantitative mineral analyses (QXRD) were conducted in the clay laboratory at Chevron-Texaco in Houston, Texas with the aid of Dr Douglas McCarty and his staff. Samples were prepared and analyzed following the methods of Srodon et al. (2001). Zincite was used as the internal standard due to its strong and conveniently located peaks

(Srodon et al., 2001). Two x-ray diffraction units were used: a Bruker Axes-D8 Advance equipped with a fifteen sample holder and a Siemens Diffraktometer D5000 equipped with a 40 sample holder, both having a theta-theta goniometer, and a Kevex Peltier cooled silicon solid-state detector using. $\text{CuK}\alpha$ radiation was used and the applied voltage was 30kV with a 30mA current. All samples were scanned from 5° to 65° 2θ at 0.02 steps at 2 seconds per step. Quantitative mineral analysis and quantitative illite polytype measurements were determined based on the Reitveld method and Autoquan (McCarty, 2002). Accuracy of Autoquan used in previous study is approximately $\pm 2\%$ of the amount present for each mineral (McCarty, 2002). The accuracy determination does not apply perfectly to our analyses because the mineral structural models used in Autoquan do not correspond exactly to the structures in our samples (McCarty, personal communication, 2005).

Semi-Quantitative Interpretations of Qualitative Mineral Analysis

A calibration curve was developed from the data obtained by the quantitative mineral analyses described above to estimate quartz to illite ratios from XRD analyses conducted in the XRD lab at The University of Montana (Figure 3). The ratio of quartz to illite determined by quantitative analyses for each sample was plotted against the relative intensities of the quartz (100) and the illite (060) QXRD peaks of each sample to create a semi-quantitative calibration curve. The intensity ratio of the quartz (100) peak to the illite (060) peak from the bulk random diffraction patterns obtained in the Clay Laboratory in the Geology Department at the University of Montana were then plotted on the calibration curve to estimate the relative proportions of quartz and illite for

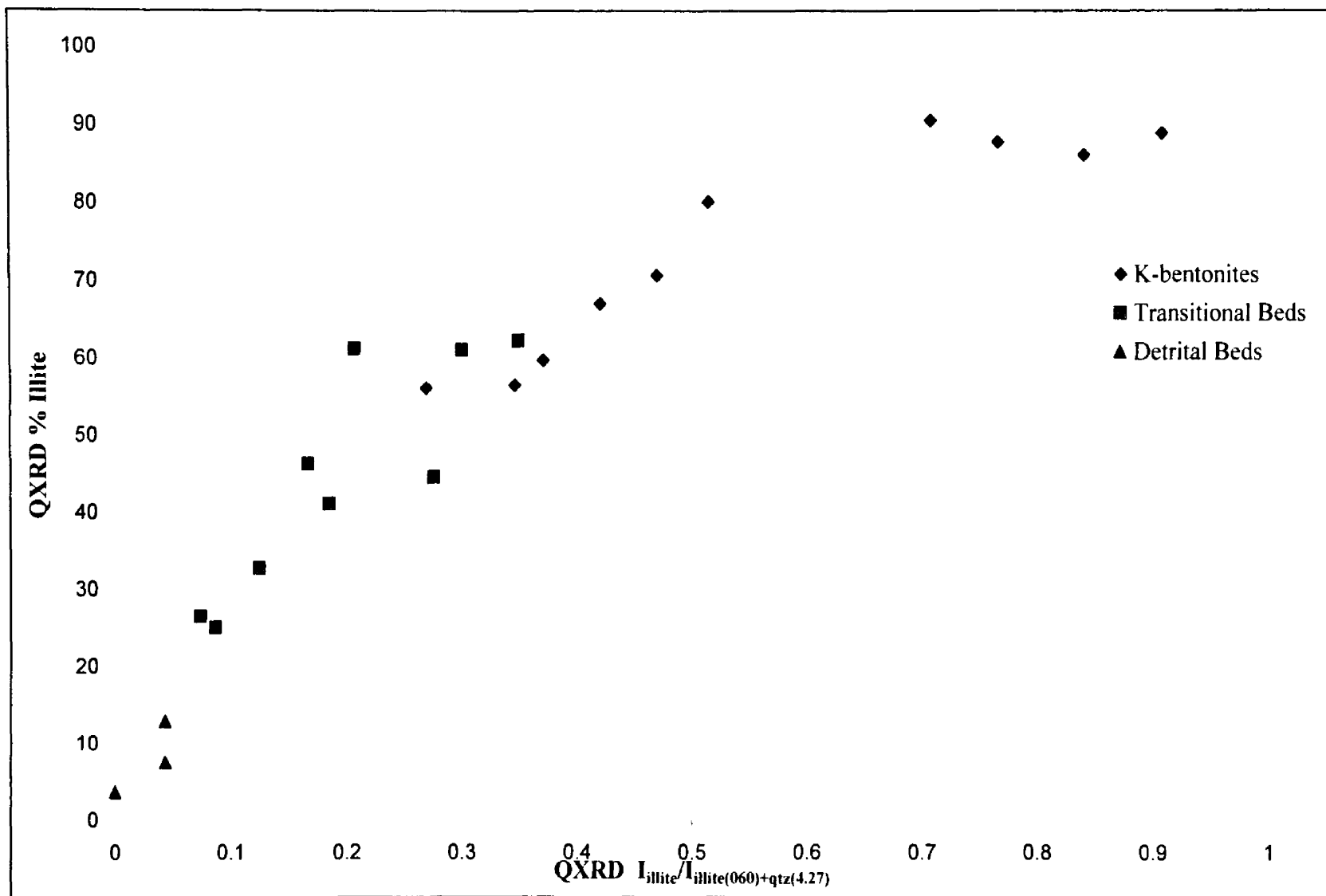


Figure 3: Calibration curve for semi quantitative interpretations of qualitative mineral analysis.

samples that were not analyzed by QXRD. This approach to estimating quartz to illite ratios is valid for many samples because quartz and illite comprise more than 95 percent of the minerals in most samples.

Chemical Analyses

Major and trace element analyses of 13 bulk samples of Belt K-bentonites were performed by XRAL Laboratories Toronto, Canada using X-ray fluorescence (XRF). The analyses are listed on Table 2. Analytical precision as determined by XRAL Laboratories Toronto, Canada is in Table 2.

Thermogravimetric Analysis (TGA)

Thermogravimetric analysis was conducted on three K-bentonites in the Clay Laboratory at Chevron Texaco following procedures of Srodon et al (1990).

Scanning Electron Microscopy (SEM)

Scanning electron microscopy was conducted at the SEM laboratory at Chevron Texaco via a Philips model XL-20 scanning electron microscope (SEM) equipped with an EDAX energy-dispersive spectrometer (EDS) on one Belt K-bentonite sample.

CHAPTER 4

RESULTS

Field Characteristics

On an outcrop scale, K-bentonites in the Belt have two different characteristic outcrop appearances, recessive beds and non-recessive beds. The recessive beds are of two types: chalky beds that exhibit inclined cleavage to bedding, i.e. asymmetric crenulation cleavage (Figure 4a & 4b) (Sears personal communication, 2004); and chalky beds that do not exhibit asymmetric crenulation cleavage (Figure 5a and 5b). One chalky K-bentonite from the upper Bonner Formation near Libby, Montana contains contorted siltstone layers ripped from the adjacent beds, suggestive of internal shearing in the K-bentonite during Laramide deformation (Figure 6). The non-recessive beds have a dense, cherty appearance exhibiting concoidal fracturing in outcrop (Figure 7). These cherty beds are clay-rich as shown in Table 1, p. 41 and 42, and grind to a chalky powder that resembles the “chalky” beds when crushed in a mortar and pestle.

Most Belt argillite beds are composed of graded silt-to-clay couplets 1-3 centimeters thick. The K-bentonite layers, including the “mixed” and “secondary” K-bentonite layers characteristically lack graded laminae and appear much finer grained.

Some Belt K-bentonites have a transitional contact with the overlying beds. The transitional layers are clay rich, gradually increasing in grain size and quartz content as they grade from the K-bentonite into the overlying siltstone or sandstone. These units are termed “transitional beds”. All of the K-bentonites have a sharp contact with the



Figure 4a: McNamara Formation along Hwy 200 at Rainbow Bend containing approximately 9 recessive K-bentonite beds indicated by arrows.



Figure 4b: Inclined cleavage to bedding, i.e. crenulation cleavage, in a K-bentonite from the McNamara Formation



Figure 5a: Recessive, chalky K -Bentonite without asymmetric crenulation cleavage in the lower Revett Formation along Hwy 93 one mile south of Ravalli.



Figure 5b: Close-up of the recessive, chalky K-bentonite without asymmetric crenulation cleavage in the lower Revett Formation along Hwy 93 one mile south of Ravalli.



Figure 6: “Mixed” K-bentonite in the upper Bonner Formation containing contorted siltstone ripped from the surrounding beds.



Figure 7: Non-recessive cherty K-bentonite bed located in the upper Bonner Formation, Libby, Montana.

underlying bed. Some K-bentonites in the Belt contain muscovite grains visible in hand specimen. The K-bentonites in the upper Belt contain muscovite grains oriented parallel to bedding, whereas the K-bentonites in the lower Belt contain randomly oriented muscovite grains. A K-bentonite, MF4031, in the Wallace Formation (Piegan Group) along highway 93 contains 4mm thick laminations of alternating light and dark colors.

Although no K-bentonite in the Belt Supergroup has been regionally correlated in this study, we expect that future work will show that at least some are regionally continuous and that some may be correlated among the modern North American, Siberian, and Australian fragments of the middle Proterozoic supercontinent on which the Belt Supergroup was deposited. The upper Wallace Formation (Piegan Group) contains a K-bentonite in two different geographic locations, one in Glacier National Park along Going-to-the-Sun-Road and one at mile 91 along highway 93 that may be the same stratigraphic unit.

Petrography

The Belt K-bentonites are very fine-grained, with clay matrix-supported quartz, feldspar, opaque minerals (possibly magnetite or ilmenite), hematite, and high relief non-opaque minerals that are most likely zircon, but are too fine-grained for conclusive petrographic identification. Quartz and feldspars are angular, sub-angular, and few are sub-rounded; some contain fluid inclusions. Quartz grains are rarely euhedral, and are commonly angular and shard like or polycrystalline. Feldspars include albite and K-spar.

Photomicrographs of selected Belt K-bentonites, Nama bentonites, and Ordovician K-bentonites are described below. All “estimated” mineral compositions are

based on petrographic estimation; QXRD data for mineral compositions are listed in Table 1 on pages 41 and 42.

Garnet Range Formation:

Figure 8 is a photomicrograph of a K-bentonite, MF6031, showing fine grained clay rich matrix supporting rounded muscovite flakes. The estimated mineral composition is 80% clay, 15% mica, 3% qtz, <2% opaques and high relief minerals. The clay matrix has a fabric that exhibits parallel extinction. Micas are rounded with very high interference colors. Quartz is rare, but elongate and angular when seen.

Figure 9 is a photomicrograph of a “mixed” K-bentonite, MF7036, showing an angular albite grain supported in a clay rich matrix. The estimated mineral composition is 85% clay, 10% qtz and feldspar, 5% opaques and non-opaques.

McNamara Formation:

Figure 10 is a photomicrograph of a K-bentonite, MF9032B, showing angular to sub-rounded grains of quartz and feldspar. The estimated mineral composition is 80% clay, 20% quartz and feldspar. Hematite staining is pervasive.

Figure 11 is a photomicrograph of a K-bentonite, MF9035 showing angular, sub-angular and sub-rounded quartz grains and a high relief mineral, most likely zircon, supported in a clay-rich matrix. The estimated mineral composition is 80% clay, 18% quartz, and <2% high relief minerals. Hematite staining is pervasive.

Figure 12 is a photomicrograph of a K-bentonite, MF90311, showing a. angular and sub-angular quartz grains containing fluid inclusions (FL), and b. showing an angular

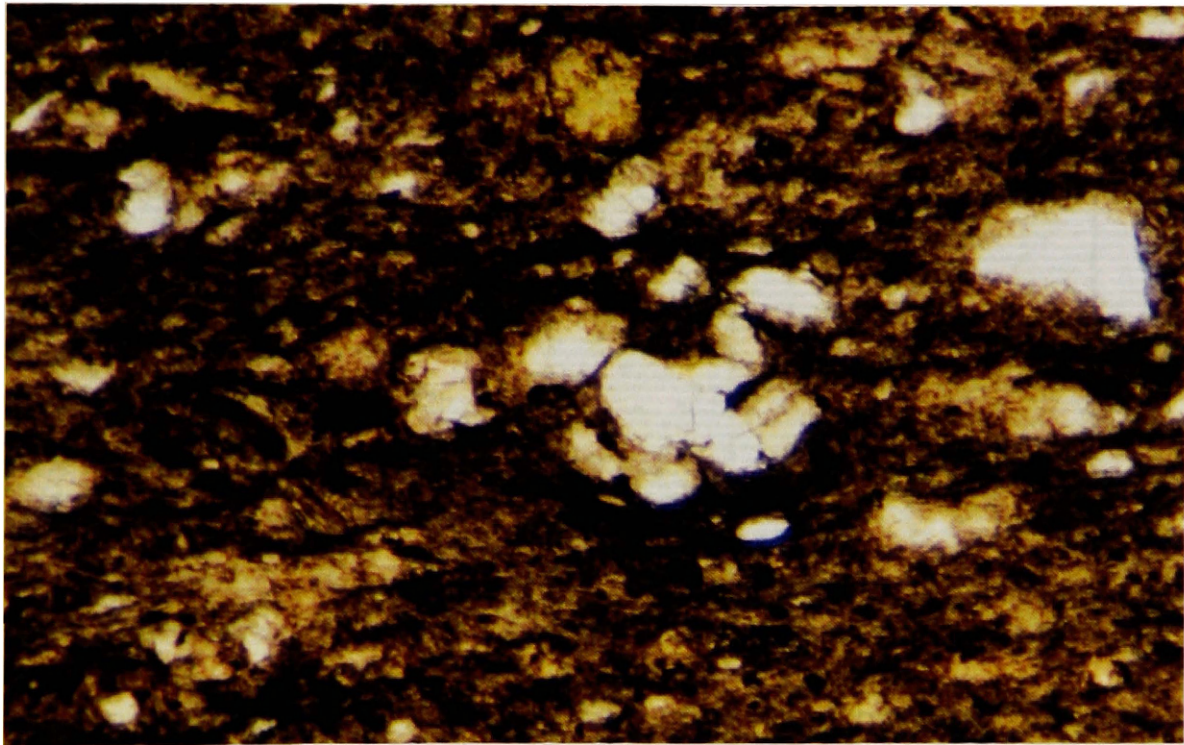


Figure 8: Photomicrograph of MF6031 from the Garnet Range Formation showing a fine grained clay rich matrix supporting rounded muscovite flakes. Scale: 16X

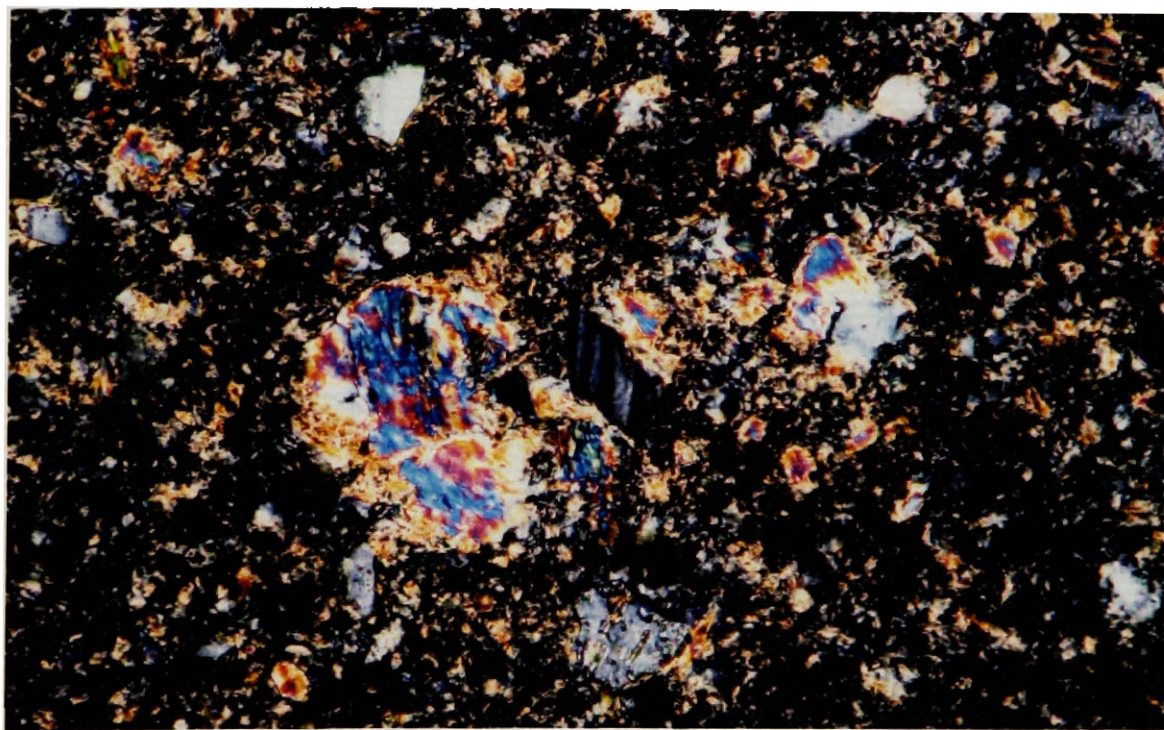


Figure 9: Photomicrograph of a K-bentonite, MF7036, from the Garnet Range Formation showing an angular albite grain supported in a clay rich matrix. Scale: 40X

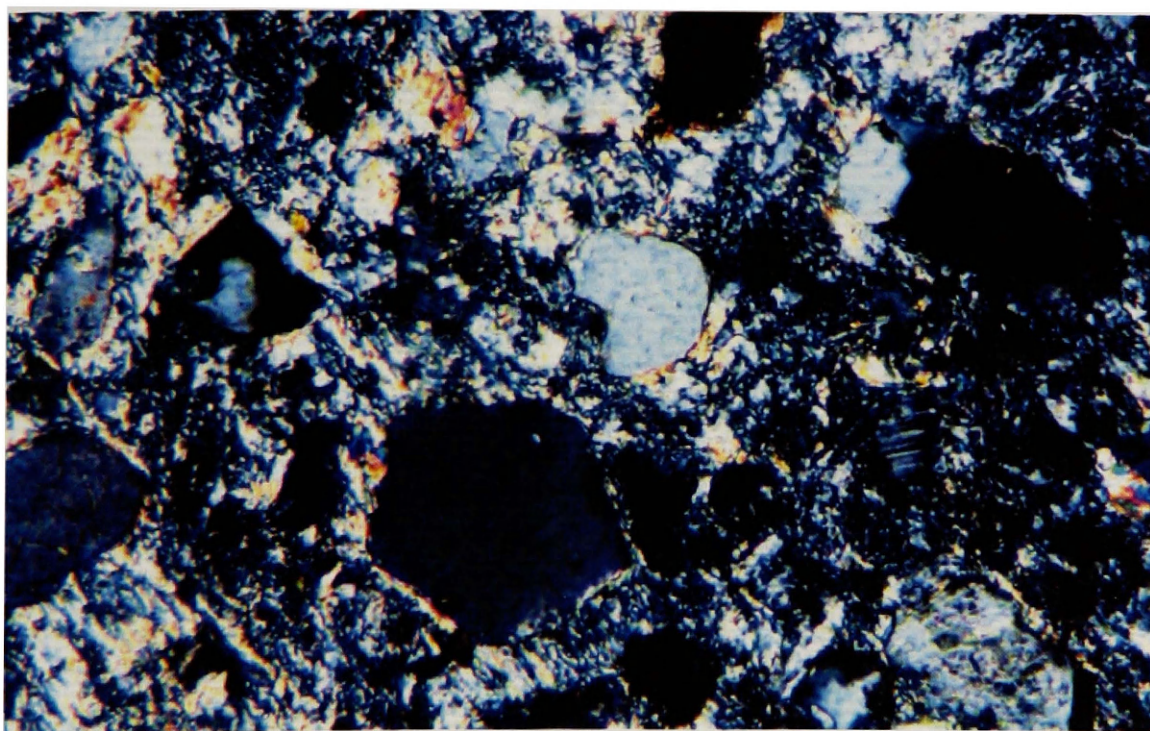


Figure 10: Photomicrograph of MF9032 from the McNamara Formation showing angular to sub-rounded grains of quartz and feldspar. Scale: 40X

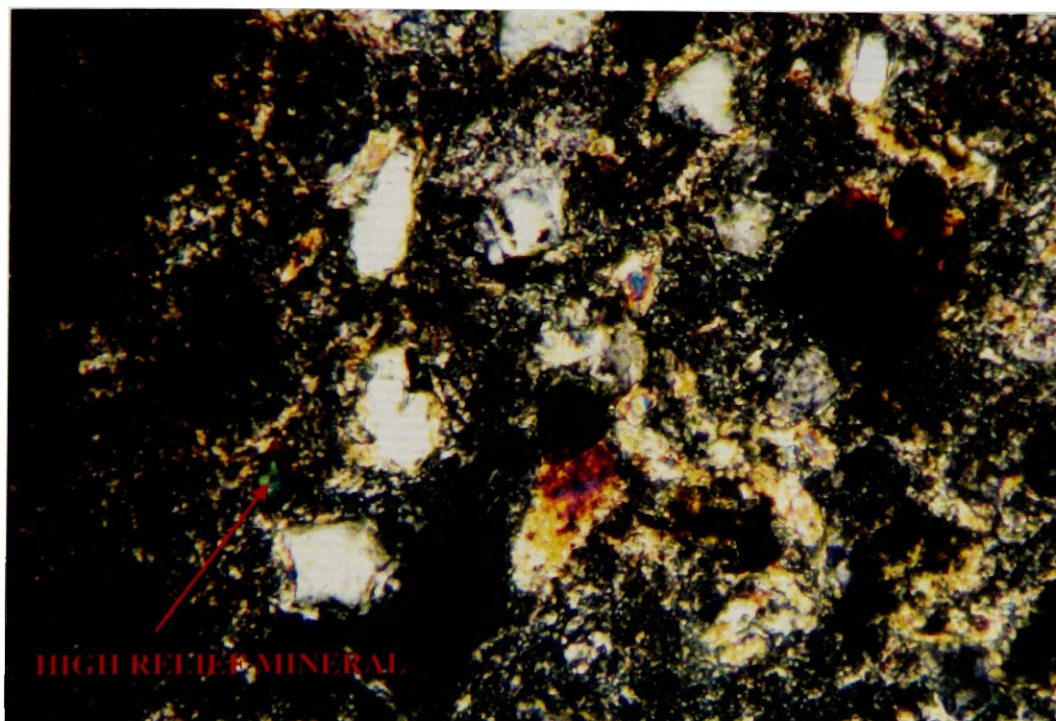
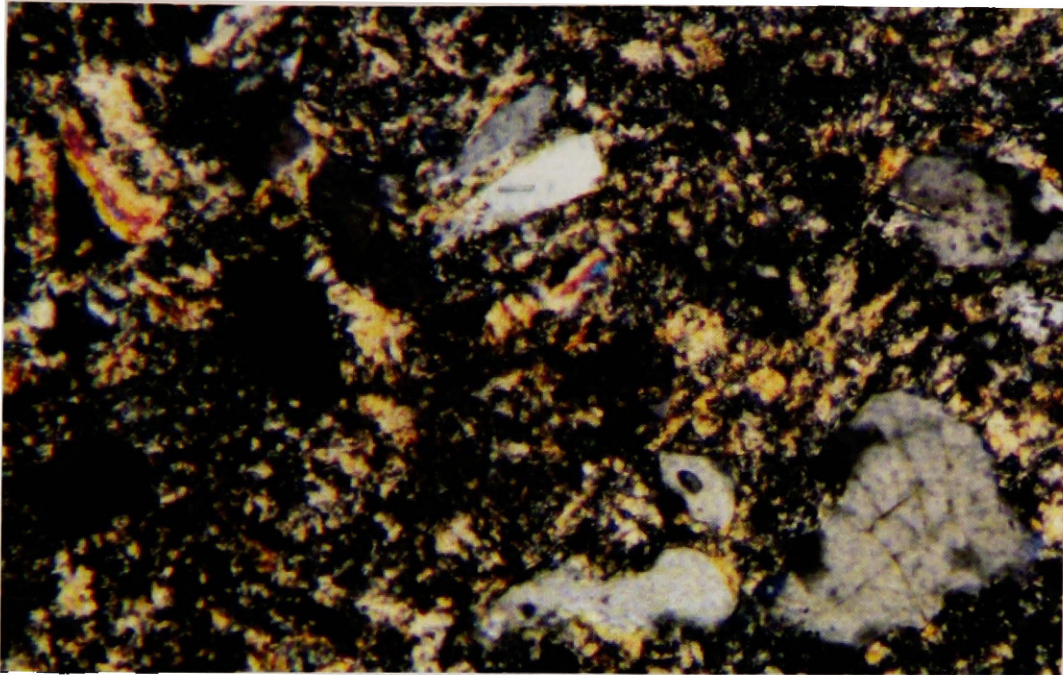
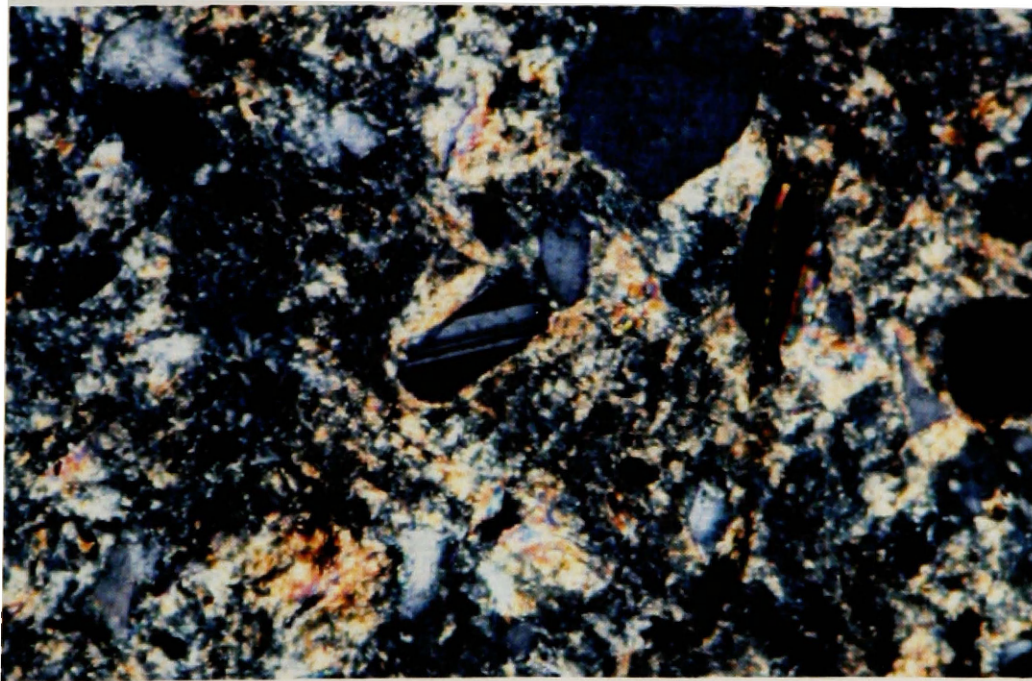


Figure 11: Photomicrograph of a K-bentonite, MF9035, from the McNamara Formation showing angular, sub-angular, and sub-rounded quartz grains and a high relief mineral, most likely zircon, supported in a clay rich matrix. Scale: 16X



12a



12b

Figure 12: Photomicrographs of MF90311 from the McNamara Formation a. showing angular and sub-angular quartz grains containing fluid inclusions (FL) and b. showing an angular albite grain supported by a clay matrix. Scale: 63X, 40X, respectively.

albite grain supported by a clay matrix. The estimated mineral composition is 65% clay, 20% quartz and feldspar, 15% opaques and heavy minerals, < 1% mica. There is no preferred orientation of platy minerals.

Figure 13 is a photomicrograph of a K-bentonite, MF90320, showing well-rounded 'balls' of clay indicating transport by water (Nanson et al., 1986). The estimated mineral composition is 85% clay, 10% quartz and feldspar, and some opaques.

Upper Bonner Formation (Missoula Group):

Figure 14 is a photomicrograph of a K-bentonite, MFBonlib, showing a fine-grained clay rich rock containing some opaques and few quartz or feldspar grains. The estimated mineral composition is 85% clay, <5% quartz, 10% high relief minerals and opaques.

Siyeh Limestone (Piegan Group):

Figure 15 is a photomicrograph of a K-bentonite, MFGoldich, showing an euhedral high relief non-opaque mineral, most likely zircon. The estimated mineral composition is 90% clay, < 2% mica, <5% quartz, <3% opaques and high relief minerals, most likely zircons. Quartz grains are elongate, angular to sub-angular and shard-like. Platy minerals are randomly oriented.

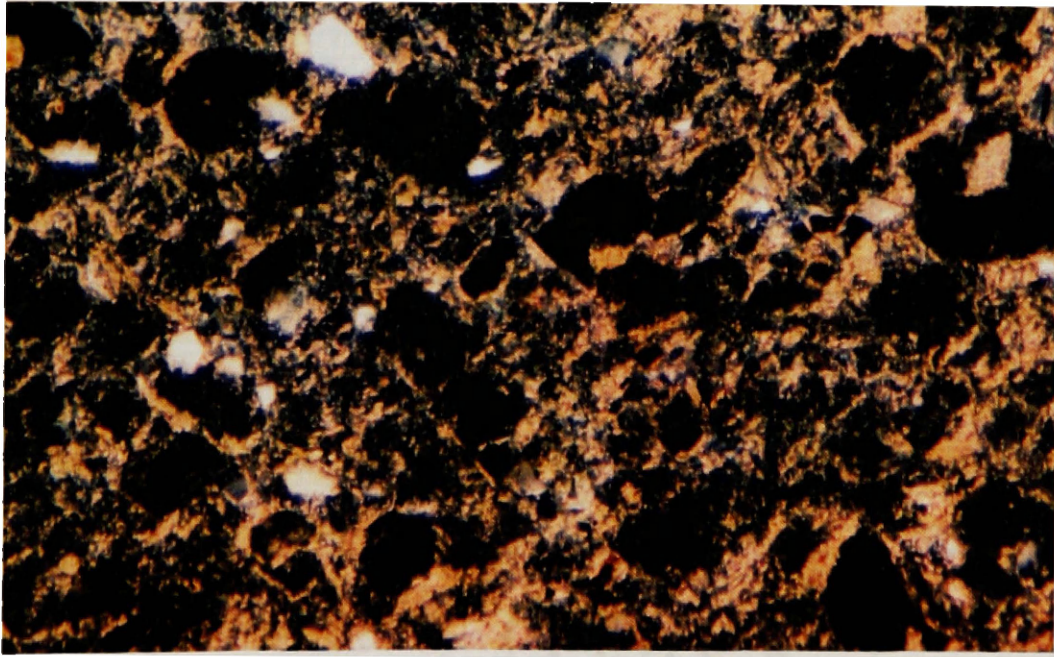


Figure 13: Photomicrograph of MF90320 from the McNamara Formation showing well-rounded “balls” of clay indicating transport by water (Nanson et al., 1986). Scale: 40X

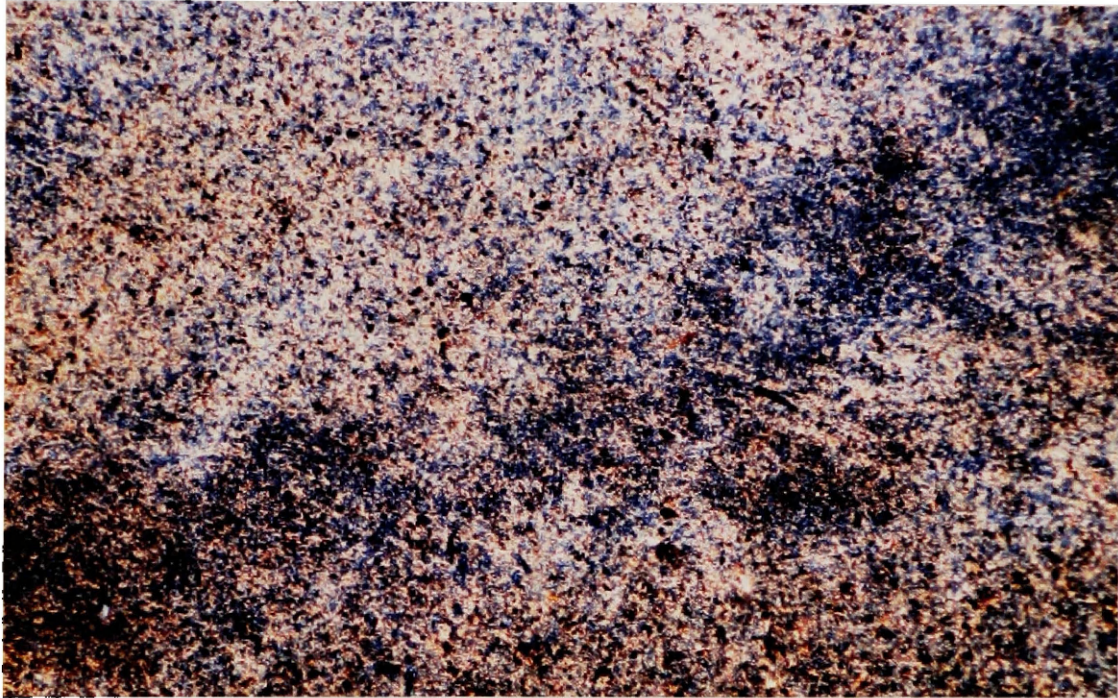


Figure 14: Photomicrograph of MFBonlib from the upper Bonner Formation showing a fine-grained clay rich rock containing some opagues and few quartz or feldspar grains. Scale: 10X

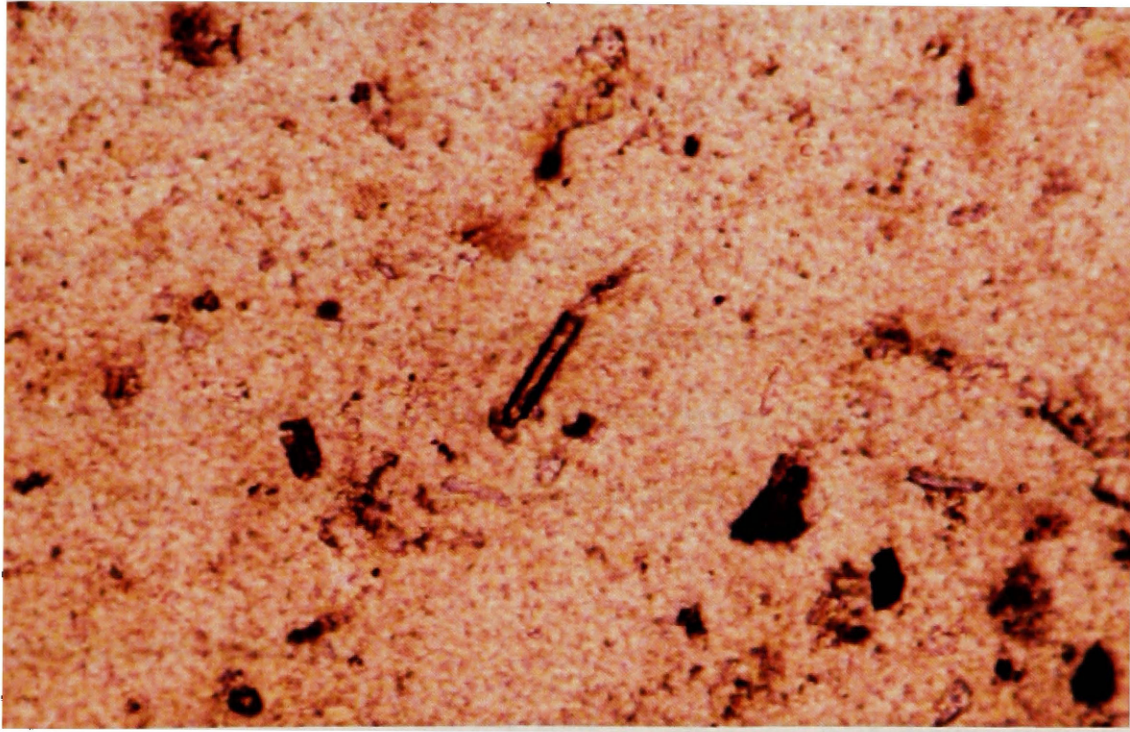


Figure 15: Photomicrograph of MFGoldich from the Wallace Formation showing a euhedral high relief non-opaque mineral, most likely zircon.
Scale: 40X

Revelt Formation (Ravalli Group):

Figure 16 is a photomicrograph of MF1031B showing polycrystalline quartz grains in a fine-grained clay rich matrix. The estimated mineral composition is 70% clay, 15% quartz and feldspar, 15% opaques, possibly magnetite or ilmenite, and high relief minerals, possibly zircons. The sample is very fine grained, with lath shaped clay matrix showing parallel extinction. The non-polycrystalline quartz is angular to sub-angular. Opaques are size sorted, which may be a result of suspension settle out.

Proterozoic Nama Supergroup K-bentonite:

Figure 17a & b are photomicrographs showing general textures of Neo-Proterozoic K-bentonites from the Nama Supergroup, Namibia (c/o Dr. Beverly Saylor). Quartz grains are angular to sub-rounded in figure 14a but are very angular in figure 14b.

Ordovician K-bentonite:

Figure 18 are photomicrographs of Ordovician K-bentonites from the Appalachian Basin (c/o Dr. Warren Huff). Angular to sub-angular grains are supported by a fine-grained clay rich matrix.

Transitional Beds:

The transitional beds are coarser grained than the underlying K-bentonites. They contain angular, sub-angular, sub-rounded, rounded and shard-like quartz and feldspar grains that are not in grain to grain contact. Polycrystalline quartz was identified

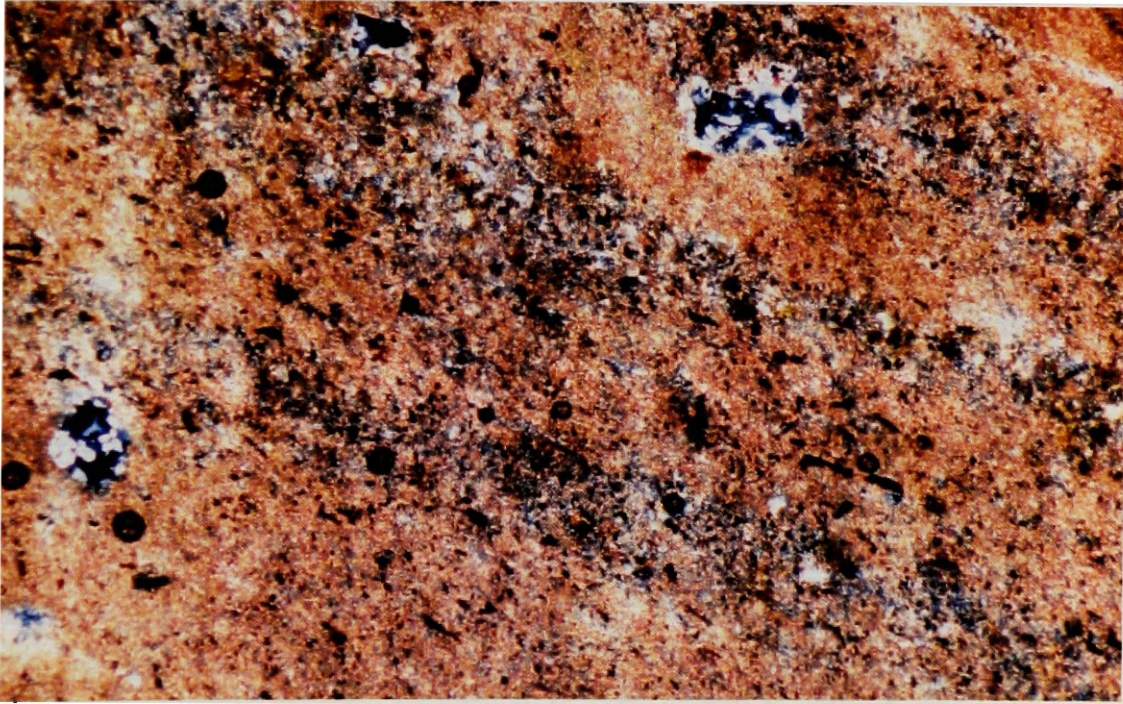
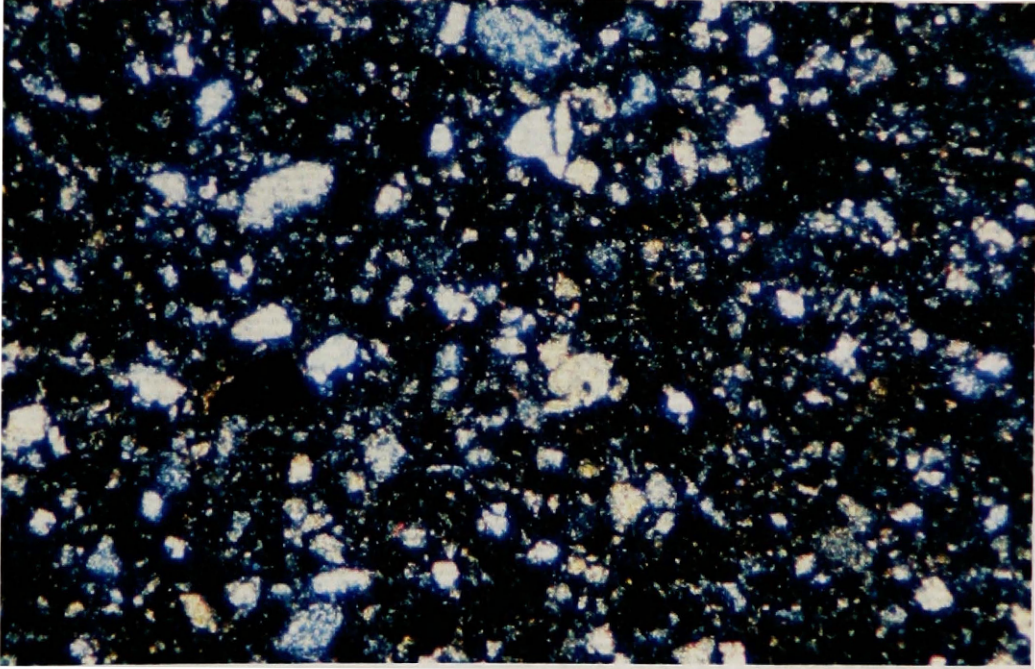
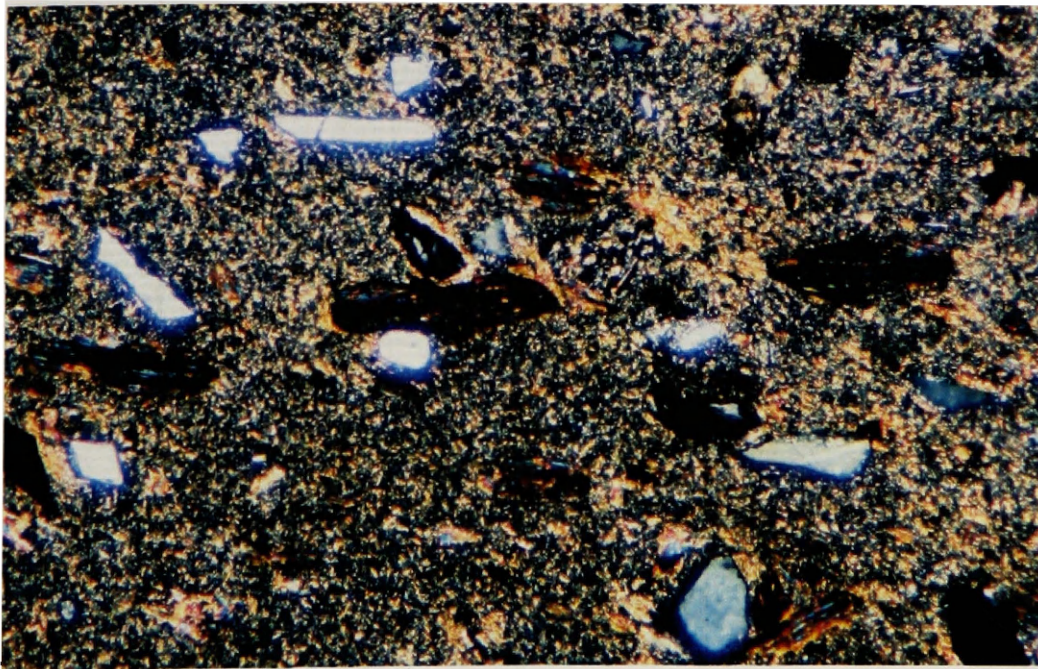


Figure 16: Photomicrograph of MF1031B from the Ravalli Formation showing polycrystalline quartz (P) grains in a very fine-grained clay rich matrix. Scale: 10X

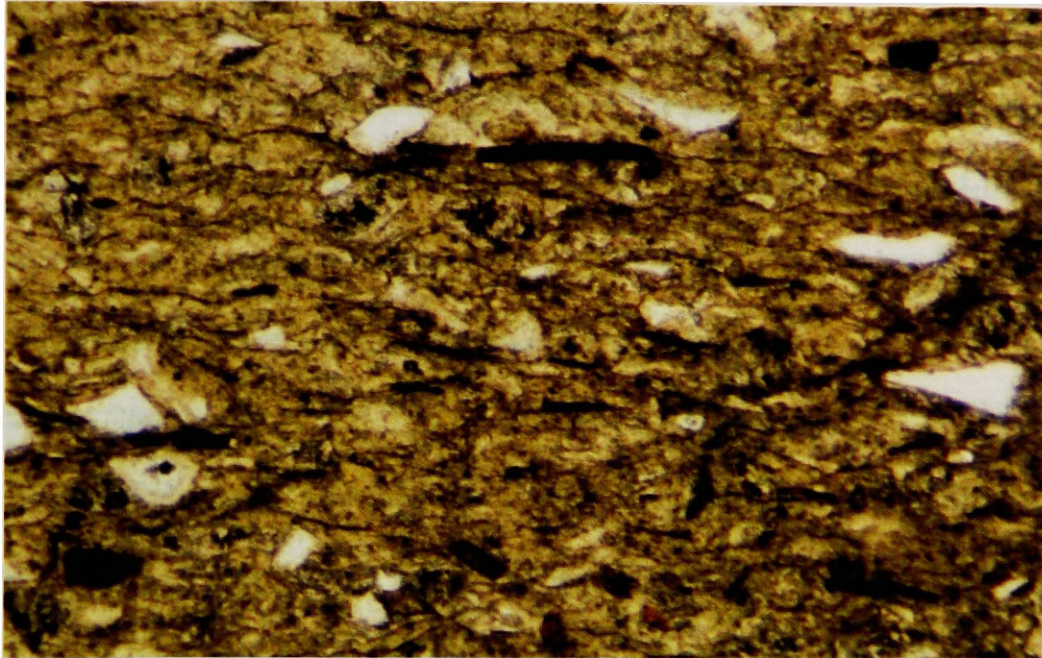


17a

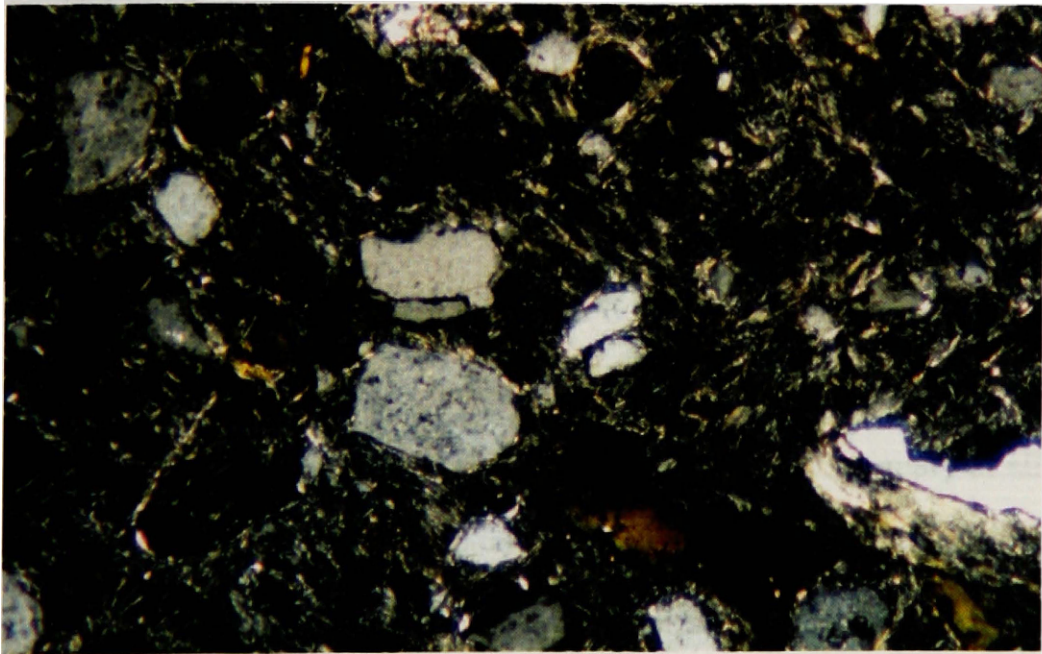


17b

Figure 17: Photomicrographs showing general textures of Neo-Proterozoic K-bentonites from the Nama Supergroup, Namibia (c/o Dr. Beverly Seylor). Quartz grains are angular to sub-rounded in figure 14a but are very angular in figure 14b. Scale: 16X



18a



18b

Figure 18a & b: Photomicrographs of Ordovician K-bentonites from the Appalachian Basin (c/o Dr. Warren Huff). Angular to sub-angular grains are supported by a fine-grained clay rich matrix. Scale: 16X

in a transitional bed in the lower Revett Formation. Some beds contain abundant opaque minerals and high relief non-opaque minerals.

Figure 19 is a photomicrograph of MF1034B, a transitional bed overlying a K-bentonite from the lower Revett Formation. Quartz grains are shard-like, angular and sub-rounded. The estimated mineral composition is 50% total clay, 35% quartz, 10% feldspar, and 5% opaques and high relief minerals.

Detrital Beds:

The detrital beds are coarse grained and show grain-to-grain contact of angular, sub-angular and rounded quartz grains with some albite grains. Other detrital beds have equigranular suture textures. Opaque and high relief minerals are present, and are abundant in the bounding beds from the lower Revett Formation.

Figure 20 is a photomicrograph of MF1035, a detrital bed from the lower Revett Formation, showing suture textures of quartz grains and an albite grain with little clay matrix. The estimated mineral composition is 90% quartz, 5% feldspar, and 5% clay.

X-Ray Diffraction Analyses

All XRD patterns are presented in Appendix A. A summary of all data is presented in Table 1 on pages 41 and 42. All K-bentonite samples are dominated by illite and quartz. The illite is a mixture of 2M1, 1M cis-vacant, and 1M trans-vacant polytypes. Clastic siltstones, sandstones, and argillites above and below the K-bentonites are dominated by quartz and lesser proportions of illite.

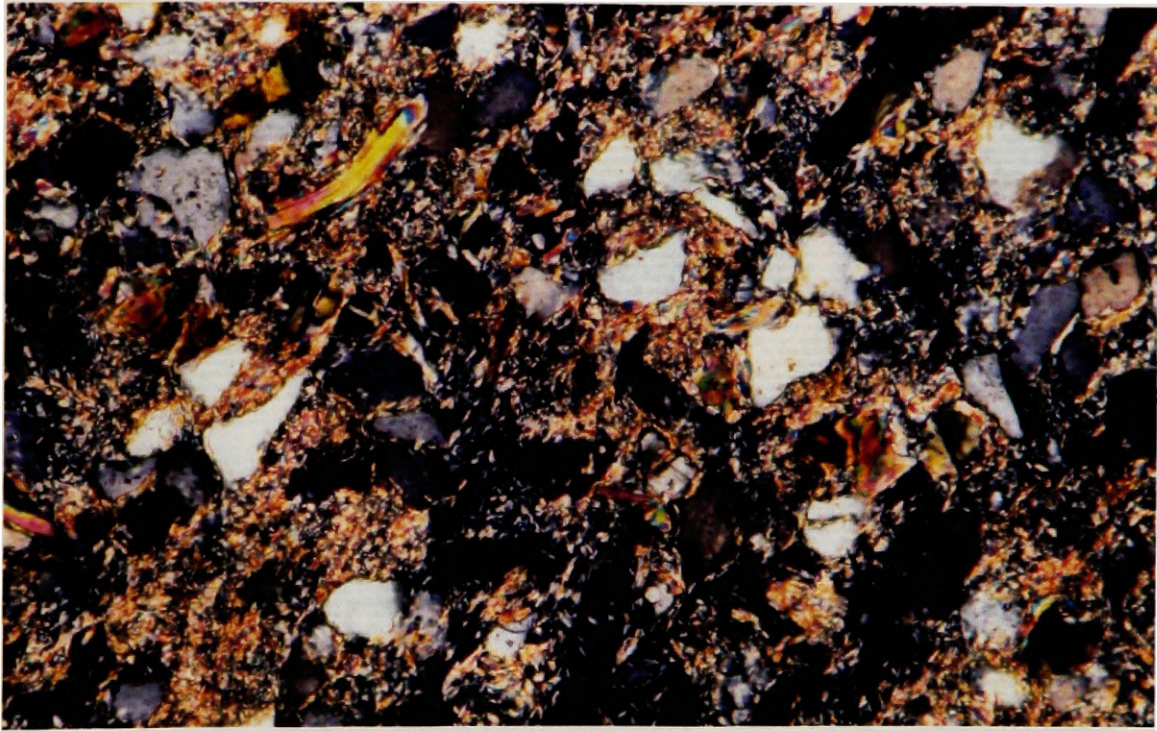


Figure 19: Photomicrograph of MF1034B, a transitional bed overlying a K-bentonite in the lower Revett Formation. Quartz textures are sherdlike, angular and sub-rounded. Scale: 40X



Figure 20: Photomicrograph of MF1035, a detrital bed from the lower Revett Formation, showing suture textures of quartz grains and an albite grain with little clay matrix. Scale: 40X

The <2 micron glycol oriented patterns of two K-bentonites, MF5031B and MF4031, contain smectite peaks at approximately 16.8 angstroms that disappear upon heating for one hour at 550°C (Figure 21 & Figure 22).

A multi-plot of the x-ray diffraction patterns of sample MF3031B shows heterogeneity within the sample bag (Figure 23). The relative intensities of the quartz (100) peak and the illite (060) peak vary considerably.

Chemical Analysis

Results of the Chemical analyses of 13 Belt Supergroup K-bentonites are presented in Table 2.

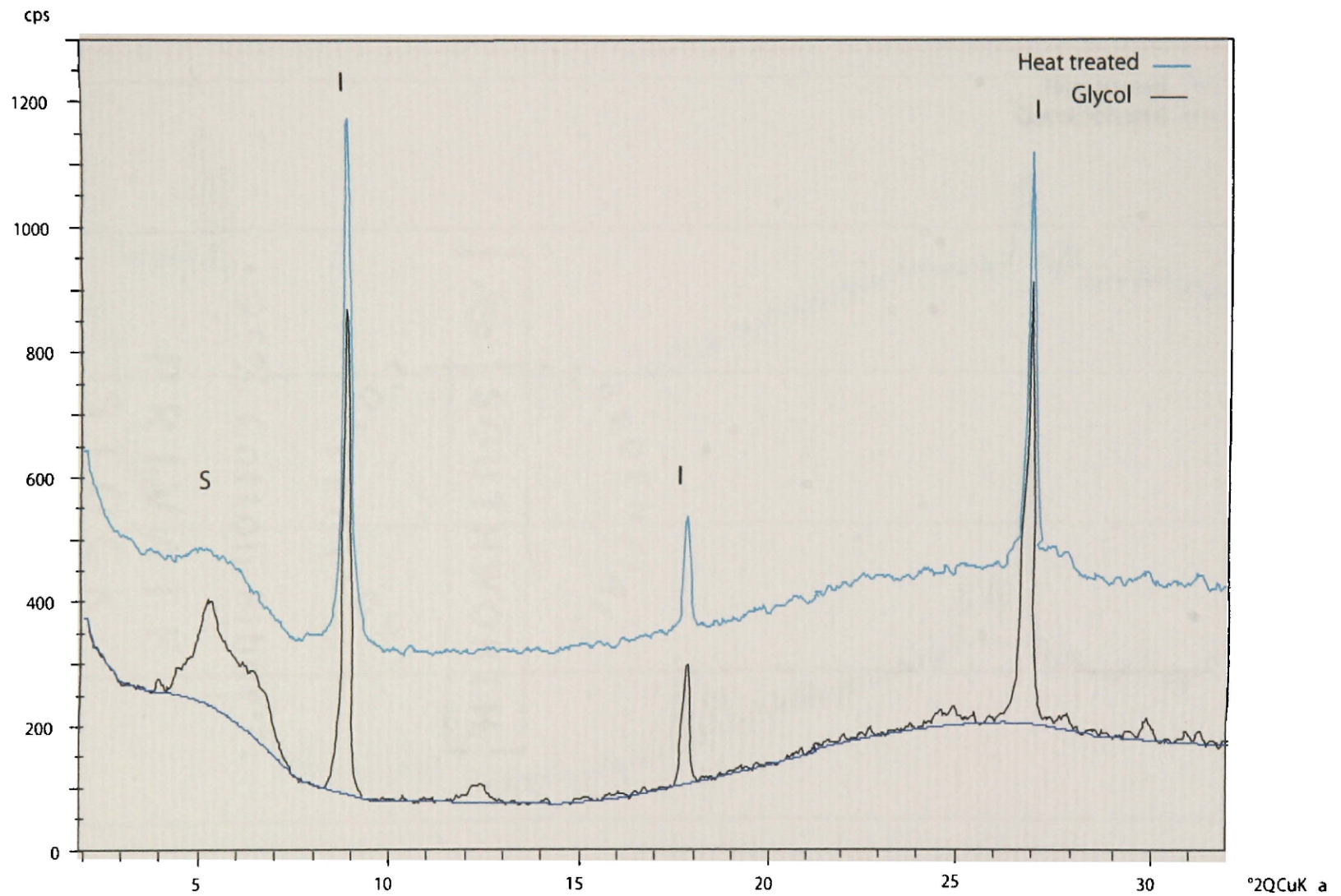


Figure 21: Multi-plot of <2> glycol solvated and heated patterns of a K-bentonite, MF5031B, from the lower Revett Formation. S=smectite, I=illite

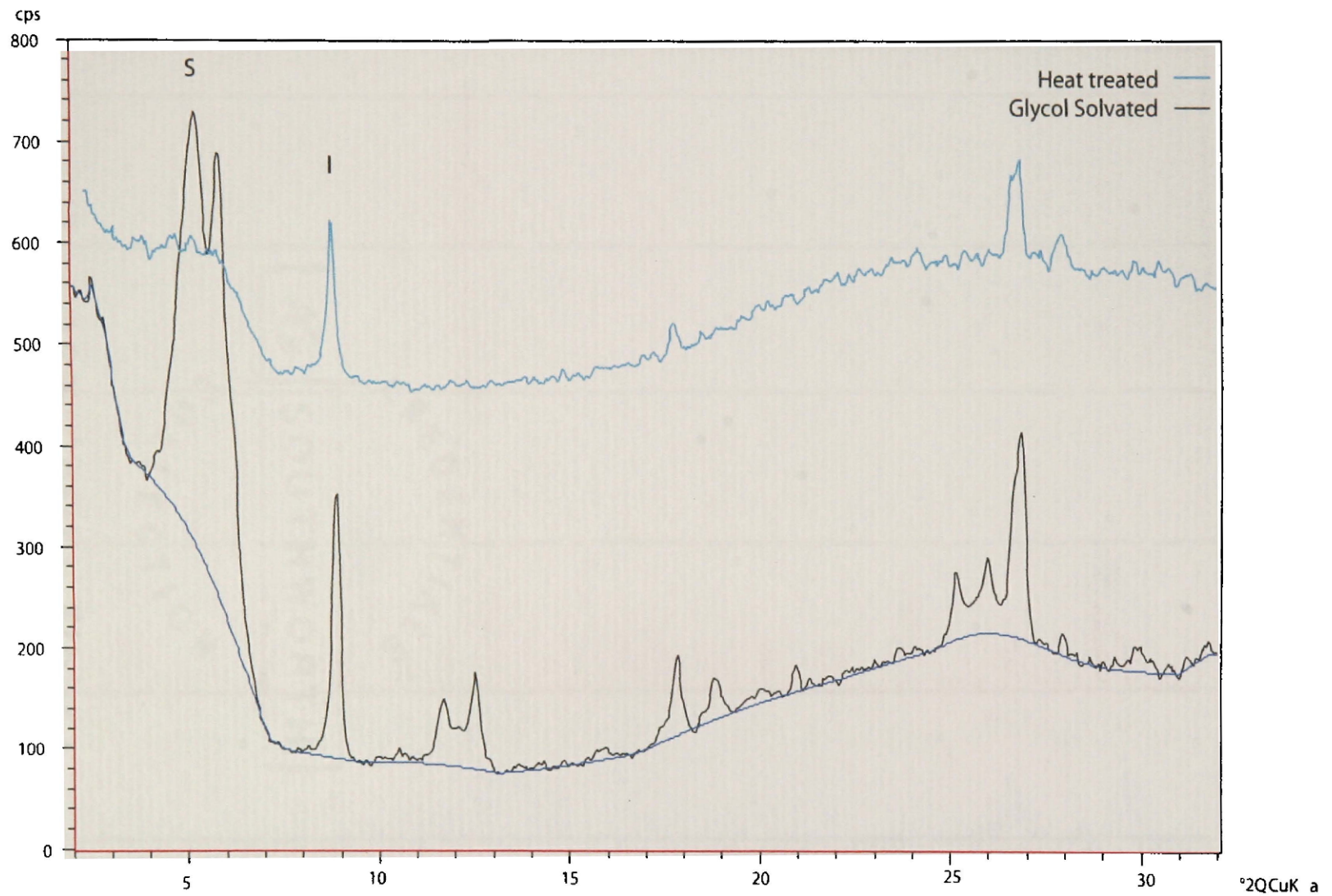


Figure 22: Multi-plot of <2 glycol solvated and heat treated patterns of a suspect K-bentonite*, MF4031B, from the Wallace Format on. S=smectite, I=illite

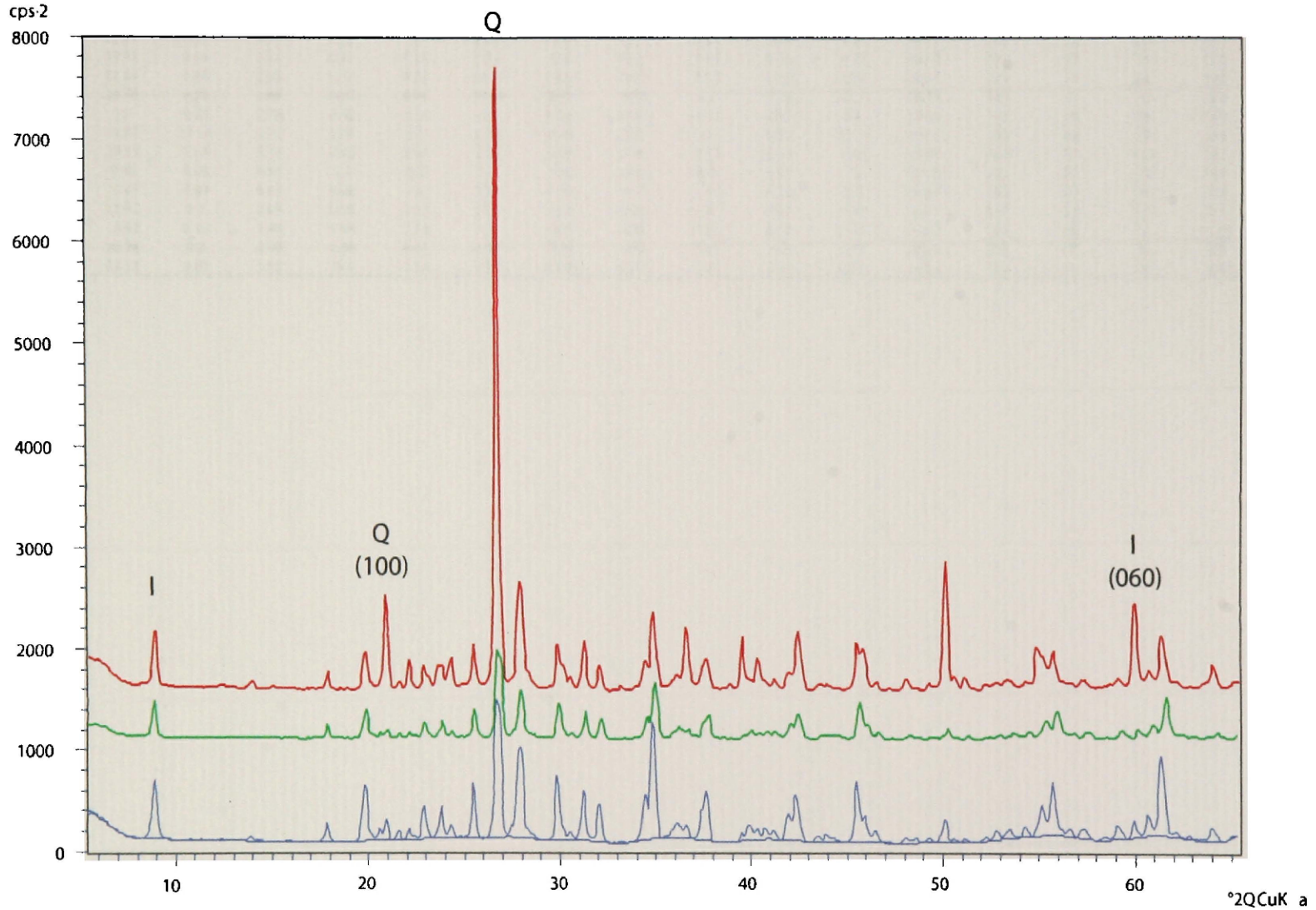


Figure 23: Random bulk rock multi-plot of K-bentonite, MF3031B, in the St. Regis Formation. Relative intensity of the illite (060) peak to the quartz (100) peak shows heterogeneity within the sample.

Table 2: Chemical analyses of 13 Proterozoic Belt K-bentonites.

Sample Id	SiO ₂ (%)	Al ₂ O ₃ (%)	CaO (%)	MgO (%)	Na ₂ O (%)	K ₂ O (%)	Fe ₂ O ₃ (%)	MnO (%)	TiO ₂ (%)	P ₂ O ₅ (%)	Cr ₂ O ₃ (%)	LOI (%)	Sum (%)	Rb (ppm)	Sr (ppm)	Y (ppm)	Zr (ppm)	Nb (ppm)	Ba (ppm)
MF6031	53.3	25.67	0.97	1.88	0.19	9	2.41	<0.01	0.84	0.64	<0.01	4.1	99.22	306	21	152	707	17	667
MF1031	60.86	19.73	0.34	2.11	0.12	7.77	3.74	0.02	0.39	0.19	0.02	4.75	100.2	306	20	35	202	16	1020
MF9035	48.72	23.04	0.48	2.82	0.13	9.38	10.37	0.06	0.63	0.15	<0.01	4.55	100.5	369	16	62	542	15	775
MF90311	47.3	23.45	0.26	2.68	0.03	9.51	10.45	0.05	0.28	0.1	<0.01	4.25	98.53	349	8	33	285	14	775
MF90317	54.21	23	0.27	2.76	0.42	9.13	5.1	0.06	0.43	0.11	<0.01	4.4	100.1	378	16	46	220	15	720
MF4037	45.17	11.07	17.13	3.79	1.01	3.1	2.72	0.03	0.37	0.07	<0.01	15.7	100.3	132	84	38	104	9	884
MF90314	55.3	23.19	0.65	2.75	0.15	8.93	3.18	0.05	0.69	0.12	<0.01	4.35	99.59	325	27	113	817	16	712
MF3031	79.95	9.92	0.08	0.91	2.1	2.52	2.2	0.02	0.52	<0.01	0.03	1.2	99.65	121	51	35	915	15	546
MF4031	63.67	15.47	0.49	6.47	0.66	4.6	3.55	0.03	0.57	0.14	<0.01	3.75	99.67	203	27	45	374	16	1520
MF9032	57.84	21.95	0.3	2.83	0.15	8.92	3.15	0.05	0.33	0.12	<0.01	4.25	100.1	349	21	55	216	15	659
MF16041	67.98	15.97	0.16	1.49	1.98	5.25	3.3	0.02	0.86	0.02	0.02	2.75	100.1	222	56	32	1150	19	866
MF5031	60.13	20.78	0.2	1.95	1.56	6.44	4.67	0.19	0.63	0.02	<0.01	3.45	100.3	265	57	76	255	17	1660
MFBonLib	55.32	24.12	0.07	1.92	0.1	9.54	4.29	<0.01	0.47	0.05	<0.01	4.25	100.4	365	8	80	500	14	980

Thermogravimetric Analysis

MF6031 (Figure 24) shows two de-hydroxylation temperatures, one above 750°C and one below 650°C, and MFBonLib (Figure 25) shows two de-hydroxylation temperature intervals above 700°C, both corresponding to cis-vacant polytype structures (Drits et al., 1995, 1998). A third K-bentonite, MF5032C, shows two de-hydroxylation temperature intervals, one above 650°C and one below 650°C (Figure 26), corresponding respectively to cis-vacant and trans-vacant structures (Drits et al., 1995, 1998). Experimental procedures involving continuous temperature rise probably caused the de-hydroxylation events to appear at temperatures at least 50° above the actual temperatures (McCarty, personal communication, 2005).

Scanning-Electron Microscopy

Figure 27 shows a K-bentonite, MF6031, from the lower Garnet Range Formation. Small illite crystals appear to have grown on the (001) surface of larger platy 2M1 muscovite. A euhedral calcite (Figure 28) crystal is also present although rare.

U-Pb Dating

Currently, Dr. Kevin Chamberlain from the Geology Department at the University of Wyoming is extracting zircons from several K-bentonites identified in the McNamara Formation and one K-bentonite identified in the Garnet Range Formation.

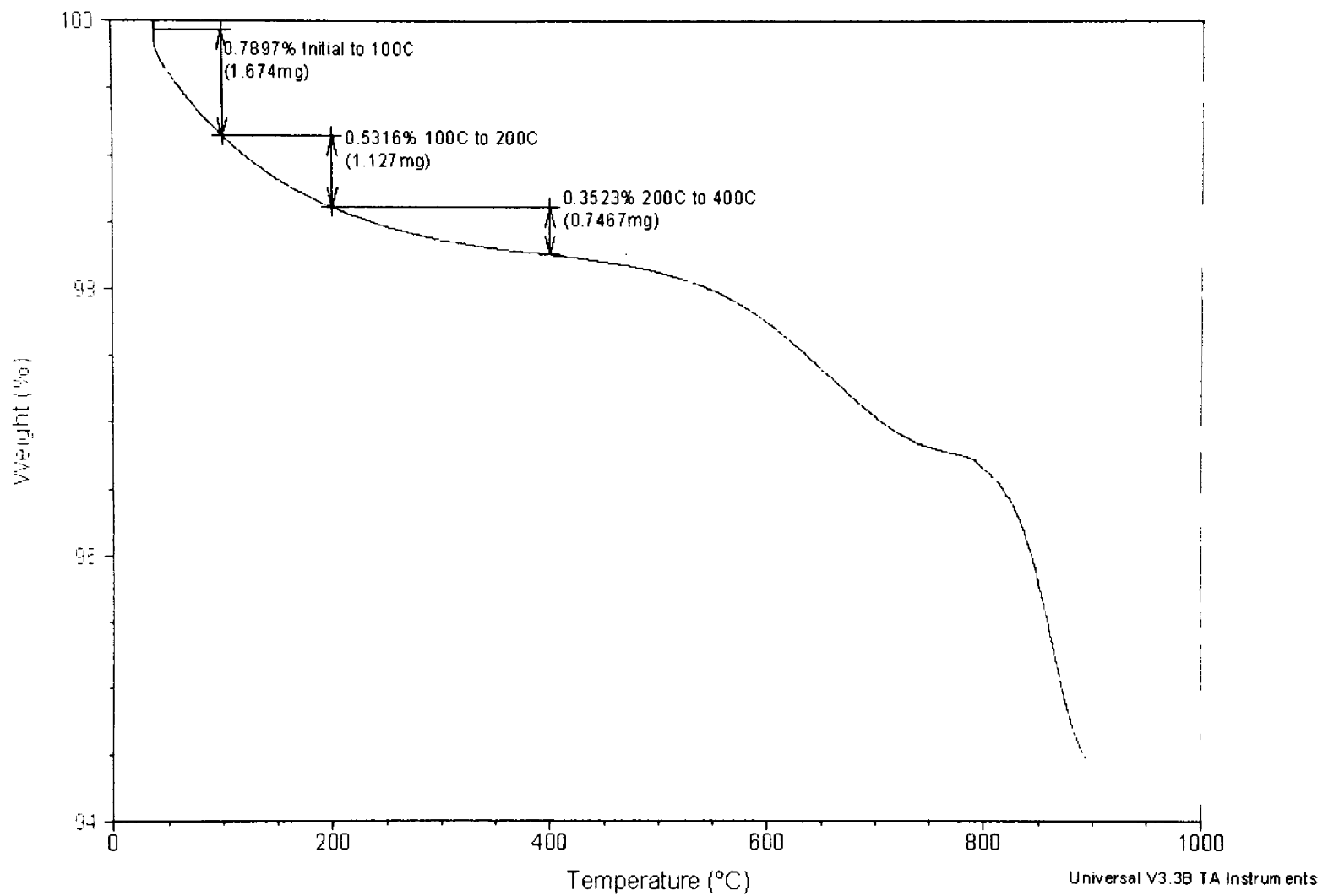


Figure 24: TGA data for MF6031 showing two de-hydroxylation temperature intervals, one below 750°C and one above 750°C.

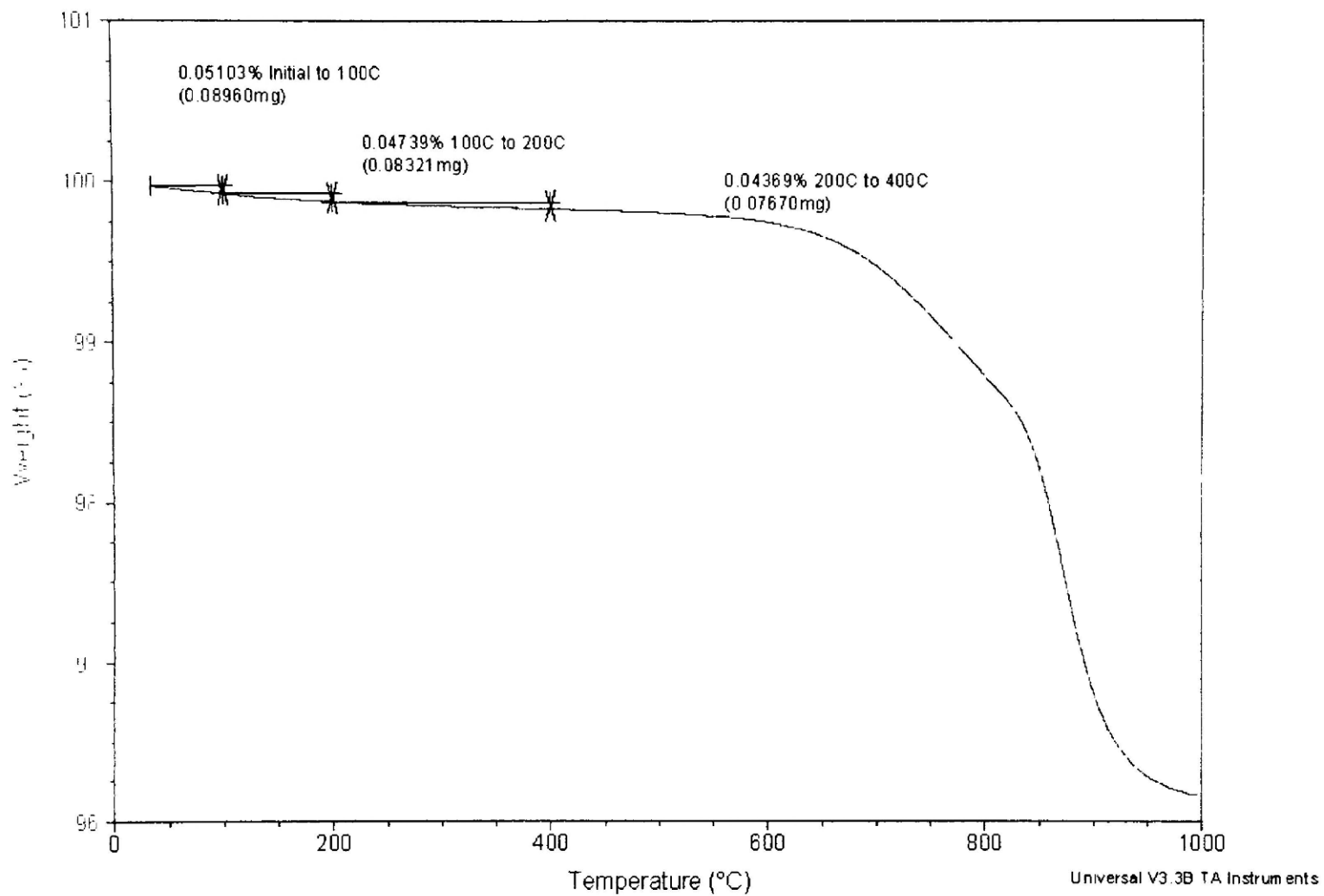


Figure 25: TGA data for MFBonLib showing two de-hydroxylation temperature intervals, both above 700°C.

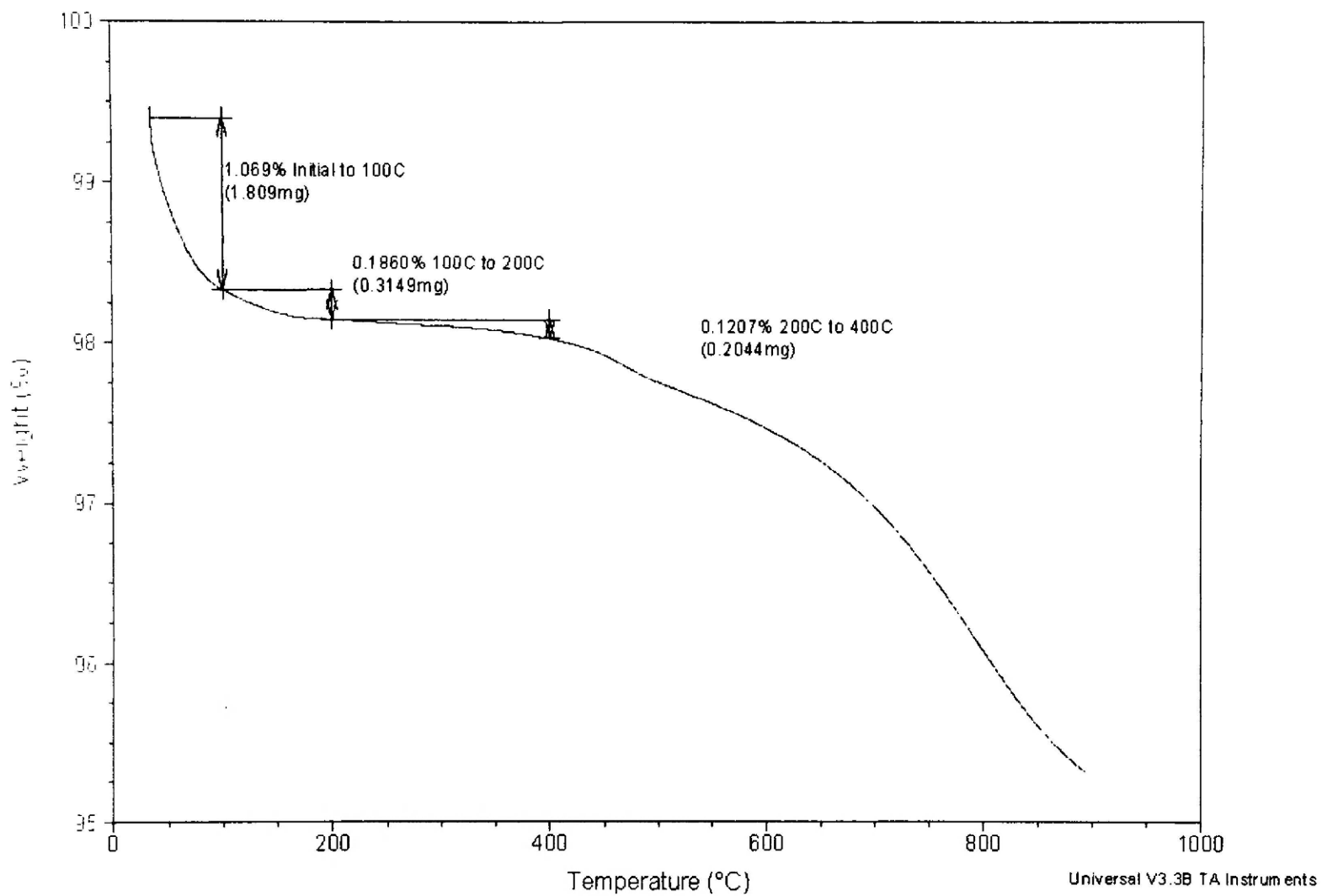


Figure 26: TGA results for MF5032C showing two dehydroxylation temperature, one below 650°C and one above 650°C.

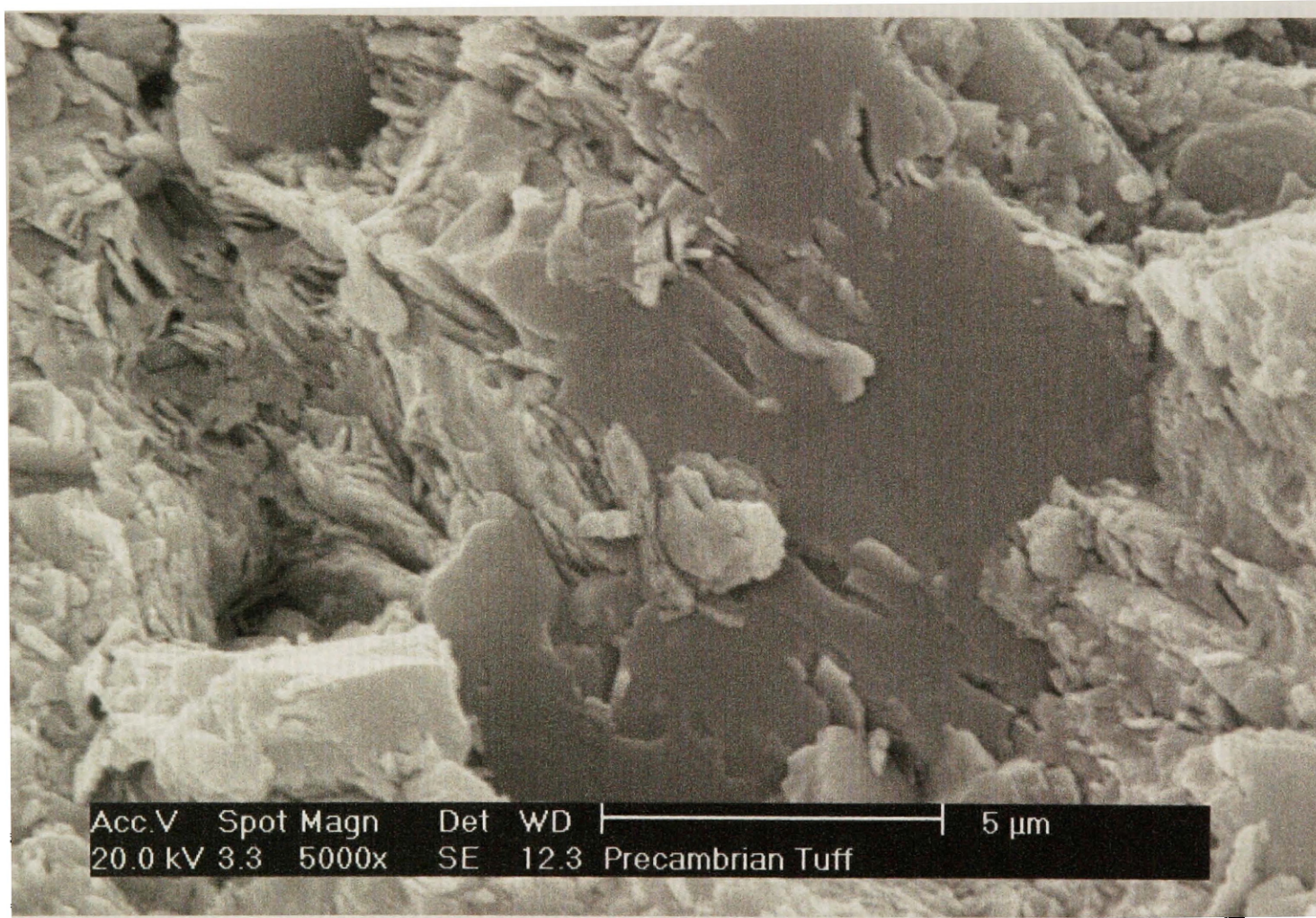


Figure 27: SEM of MF6031 showing the fine-grained textures and showing presumably illite growing from the (001) surface of a muscovite grain.

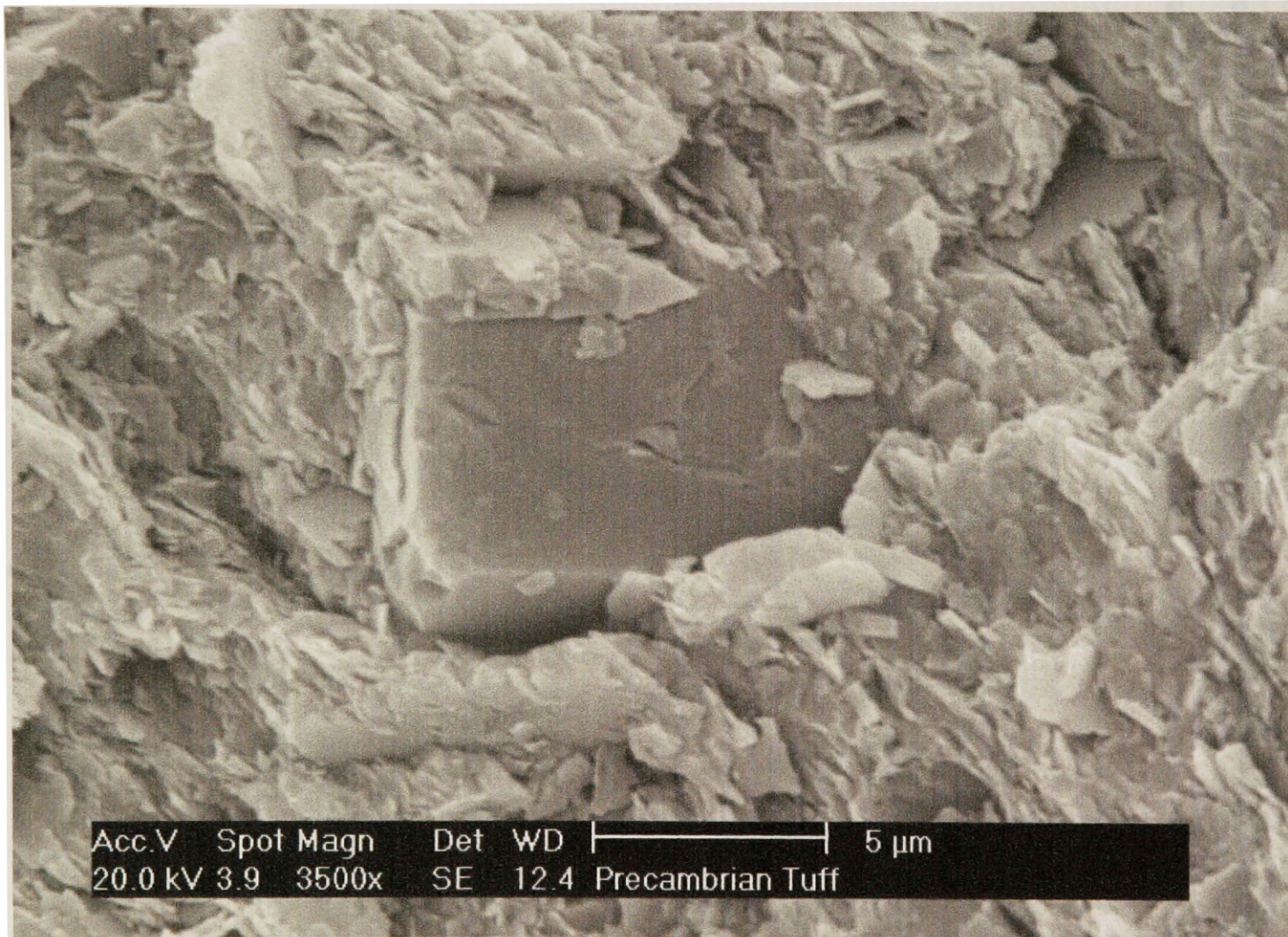


Figure 28: SEM of MF6031 showing a euhedral calcite grain supported by a very clay rich fine grained matrix.

The U-Pb date obtained thus far from one K-bentonite in the Garnet Range Formation, MF6031, yielded an age of approximately 1600 MA (Chamberlain, personal communication, 2005). This age coincides with detrital zircon ages from the Belt (Sears, in review). SHRIMP analysis will be employed to analyze individually both rounded and euhedral zircons in hopes of obtaining accurate ages of the volcanic events that formed the Belt K-bentonites.

CHAPTER 5

DISCUSSION

Recognition and Identification of Belt K-bentonites

Although there is no single “smoking gun” for the identification of K-bentonites in the Belt Supergroup, outcrop appearance, petrographic textural characteristics, mineral composition, illite polytype characteristics, and SEM textural characteristics collectively leave little doubt that felsic volcanism contributed considerable material to the Belt Supergroup, both in the form of numerous recognizable K-bentonite layers and as the considerable quantities of illite and chlorite in Belt argillites and siltites.

Belt K-bentonites have two characteristic outcrop appearances, recessive-weathering chalky textured beds and non-recessive cherty textured beds that become chalky when crushed. Some of the chalky K-bentonites show evidence of internal deformation and shearing. The K-bentonites from the McNamara Formation at Rainbow Bend on highway 200 show asymmetric crenulation cleavage and show slickenside surfaces at the contact with the underlying sandstones and siltstones (Figures 4 and 5). One chalky K-bentonite in the Bonner-Libby transitional zone near Libby Montana contains contorted siltstones that were ripped from the bounding beds and deformed into s-shaped folds, implying that the K-bentonite absorbed considerable translation between the overlying and underlying strong sandstones during Laramide deformation (Figure 6).

The textural differences between the chalky and the cherty K-bentonites may result from a process in which the chalky K-bentonites originally formed with cherty

textures, and developed their current chalky texture as a result of crushing and internal slip during Laramide deformation of Belt rocks. In this case, the cherty K-bentonites would simply have avoided internal slip and retained their earlier texture. An alternative explanation is that the chalky beds may have been deposited by flowing water or may have been reworked after initial deposition, whereas the cherty K-bentonites are the result of primary deposition of air-fall ash. However, SHRIMP analyses of zircons from the cherty K-bentonite in the upper Bonner Formation at Kootenai Falls shows mixing of both rounded zircons that yield uranium-lead ages older than the depositional age, and euhedral zircons that give depositional ages, indicating that this K-bentonite is a “mixed” or “secondary” K-bentonite (Evans et al., 2000).

As mentioned earlier, bentonites and K-bentonites have three general modes of deposition: air-fall ash settling directly into the aqueous environment and being preserved as primary sedimentary beds, reworking of primary sedimentary beds in situ via waves, tides, or currents, and terrigenous air-fall ash that was later eroded and transported into the aqueous environment by flowing water (Ver Straeten, 2004; Huff, personal communication, 2005; Hayes, 1994). The latter two types were described earlier as a “mixed” K-bentonites and “secondary” K-bentonites, respectively. A photomicrograph of one chalky sample, MF90320, from the McNamara Formation along highway 200 at Rainbow Bend shows spherical balls of clay (Figure 13). Nanson et al. (1986) interpreted similar spherical balls of mud in samples from Cooper Creek in central Australia, to have originated as mud braids that were remobilized during flooding events as sand sized pedogenic aggregates that were transported over low-gradient surfaces and preserved in sedimentary beds.

A transitional bed represented by samples MF1032, MF1033, and MF1034 overlies a K-bentonite in the lower Revett Formation, shows fine laminations and is very fine-grained and clay rich proximal to the K-bentonite. Up-section, away from the K-bentonite, the clay content decreases as the grain size and quartz content increases. This gradation probably resulted from decreasing input of detrital volcanic ash as erosion exhausted a terrigenous ash source or of air-fall ash, and a constant supply of normal detrital quartz-rich sands and silts (Huff, personal communication, Hayes, 1994).

Petrographic Data

Petrographic data are compatible with the bentonitic nature of the studied beds. Some of the Belt K-bentonites contain polycrystalline quartz that suggests post-depositional precipitation of quartz from silica released during the illitization of smectite. Angular, sub-angular, sub-rounded, and euhedral grains of quartz and feldspar are also compatible with a volcanic ash origin for the K-bentonites. Micas are rare and commonly randomly oriented suggesting in-situ growth rather than a detrital origin. Many of the high relief minerals are euhedral or angular suggesting that these grains are not of detrital origin.

The Belt K-bentonites texturally resemble K-bentonites from the Ordovician Appalachian Basin (Huff et al., 1997) and from the Neo-Proterozoic Nama Supergroup in Namibia (Seylor et al., in review). Nama K-bentonites contain few euhedral grains, and angular, sub-angular, and rounded quartz and feldspar grains, supported in a fine-grained clay-rich matrix (Figure 14). Ordovician K-bentonites also contain angular, sub-angular, and rounded quartz and feldspar grains (Figure 15).

The transitional bed, MF1033B and MF1034B, in the lower Revett Formation along highway 93 contains many of the same textures seen in the K-bentonites, such as shard-like, angular, sub-angular and rounded quartz and feldspar grains, polycrystalline quartz, as well as non-opaque high relief minerals and opaque minerals. This transitional bed records the gradual change in mineralogy and grain size as the air-fall ash supply subsided and background detrital sediments began to dominate.

Mineral Compositions

Mineralogically Belt K-bentonites are predominately composed of illite, with lesser amounts of chlorite, quartz, feldspar, and several other minerals including zircon, which is consistent with K-bentonites of other ages (Weaver, 1953; Walker, 1983; Kolata et al., 1996). Figure 29 shows quartz to clay ratios of Belt K-bentonites compared to those of Belt argillites, siltites, quartzites and carbonates (Harrison and Campbell, 1963) and Paleozoic shales (Srodon et al. 2001). It is clear that the Belt K-bentonites are mineralogically different from all other Belt lithologies in that they show substantially higher illite to quartz ratios. However, the Belt K-bentonites do show similar clay to quartz ratios to those of younger shales studied by Srodon et al. (2001). It is possible that these shales are also volcanic in origin (Thompson, personal communication, 2004; McCarty, personal communication, 2004).

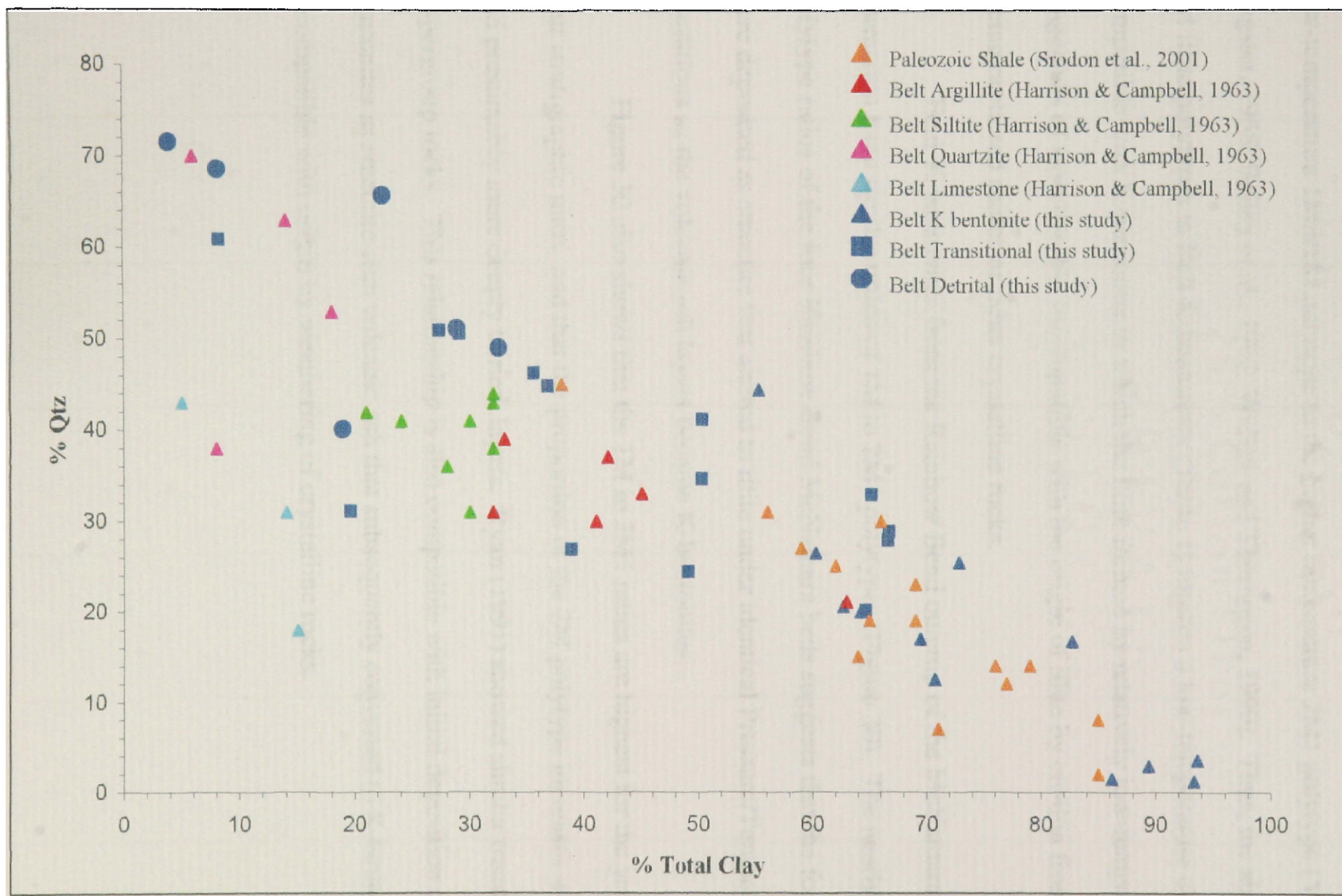


Figure 29: Plot of % total clay vs % quartz of Paleozoic shales, Belt argillites, siltites, quartzites, limestone and K-bentonites

Illite Polytypes

As metamorphic temperature increases, the illite polytype transforms from the low-temperature 1Md/1M polytype to the higher temperature 2M1 polytype (Yoder and Eugster, 1955; Bailey et al., 1962; Walker and Thompson, 1990). Thus, the abundance of 1M illite polytypes in Belt K-bentonites (Table 1) implies a low-temperature origin that is compatible with K-bentonite in which the illite formed by relatively low-temperature diagenesis of smectite, but incompatible with the origin of illite by erosion from older, metamorphosed shales or other crystalline rocks.

Four K-bentonites from the Rainbow Bend outcrop of the McNamara Formation have similar ratios of 1M to 2M1 polytypes (Figure 30). The nearly constant polytype ratios of the four Rainbow Bend McNamara beds suggests that the four units were deposited as smectite that altered to illite under identical Pressure/Temperature conditions as the volcanic ash layers became K-bentonites.

Figure 30 also shows that the 1M to 2M1 ratios are highest for the youngest Belt stratigraphic units, and that the proportion of the 2M polytype increases with older, and presumably more deeply buried, layers. Ryan (1991) showed similar trends in Belt Supergroup rocks. This relationship is also compatible with initial deposition of the K-bentonites as smectite-rich volcanic ash that subsequently converted to K-bentonite, and incompatible with origin by weathering of crystalline rocks.

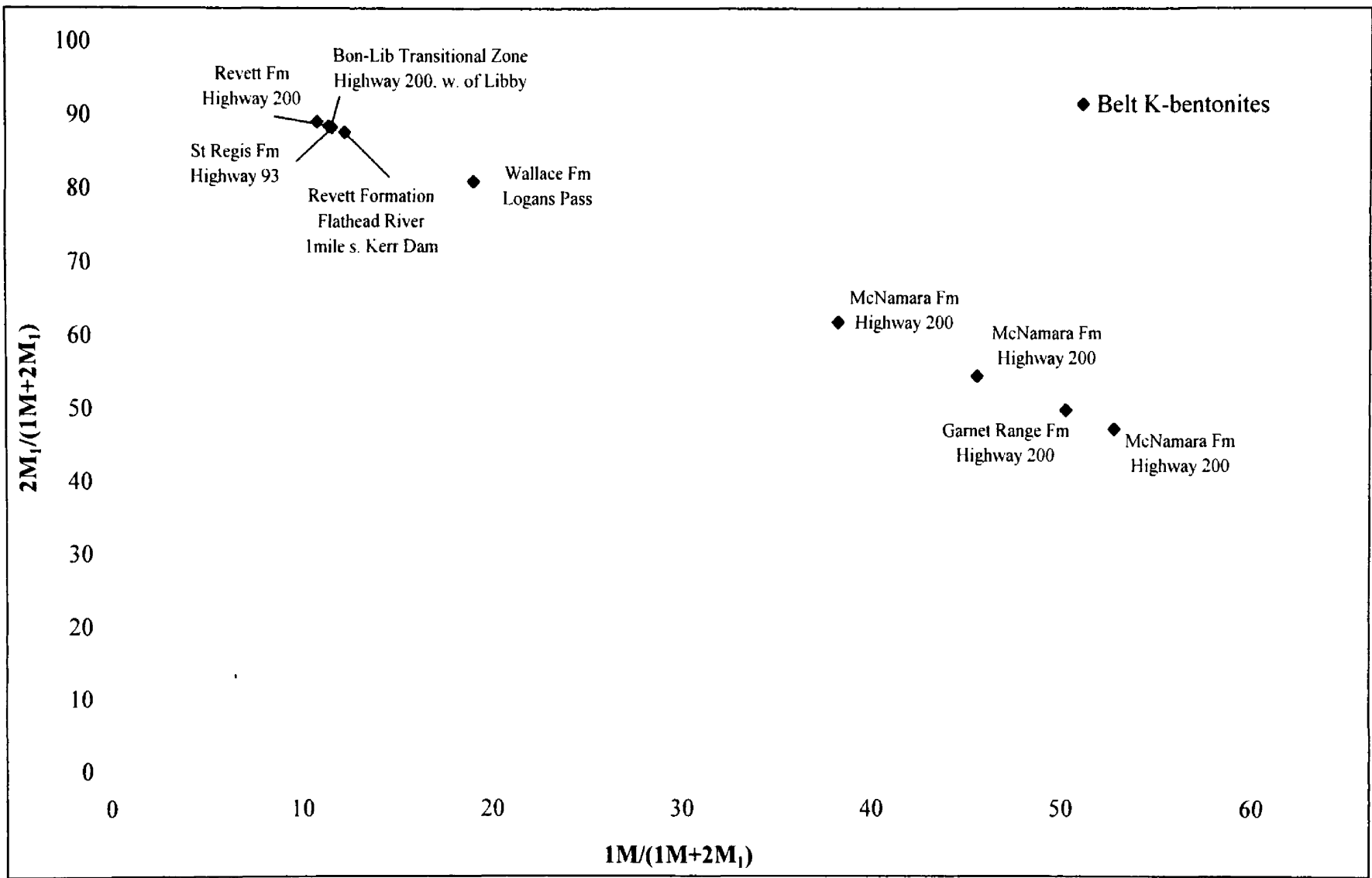


Figure 30: Plot of % 1M vs % 2M1 for K-bentonites in the Belt Supergroup.

Chemical Analyses

In marine environments, felsic volcanic ash converts to smectite as it reacts with seawater. In the process, silica, potassium, and calcium are lost from the ash and sodium and magnesium are gained as the ash becomes bentonite. During later illitization of the smectite as the bentonite converts to K-bentonite, silica is lost and potassium is gained (Walker, 1983). The chemical compositions shown in Table 2 are compatible with a felsic volcanogenic bed that has undergone this sequence of processes to form K-bentonites. It is interesting to note that the St Regis Formation, the Revett Formation, the Bonner Formation, and the McNamara Formation were deposited on alluvial aprons and therefore should not have been altered to smectite by marine waters. It is unclear as to what mechanism converted the ash in those formations to smectite.

Winchester and Floyd (1977) noted that the ratios of the relatively immobile elements Zr, TiO₂, Nb, and Y are unique for different source magmas. Nb concentrations increase with increasing alkalinity, and, as magma differentiation progresses, incompatible elements, such as Zr, increasingly concentrate in the melt (Winchester and Floyd, 1977). Following procedures of Winchester and Floyd (1977), Huff (1997) plotted Zr/TiO₂ against Nb/Y, and concluded that Osmondberg K-bentonites came from a trachyandesite source magma.

The chemical data from 13 Belt K-bentonites plot within the rhyodacite/dacite and rhyolite fields (Figure 31). These data are consistent with a felsic volcanic source for Belt K-bentonites.

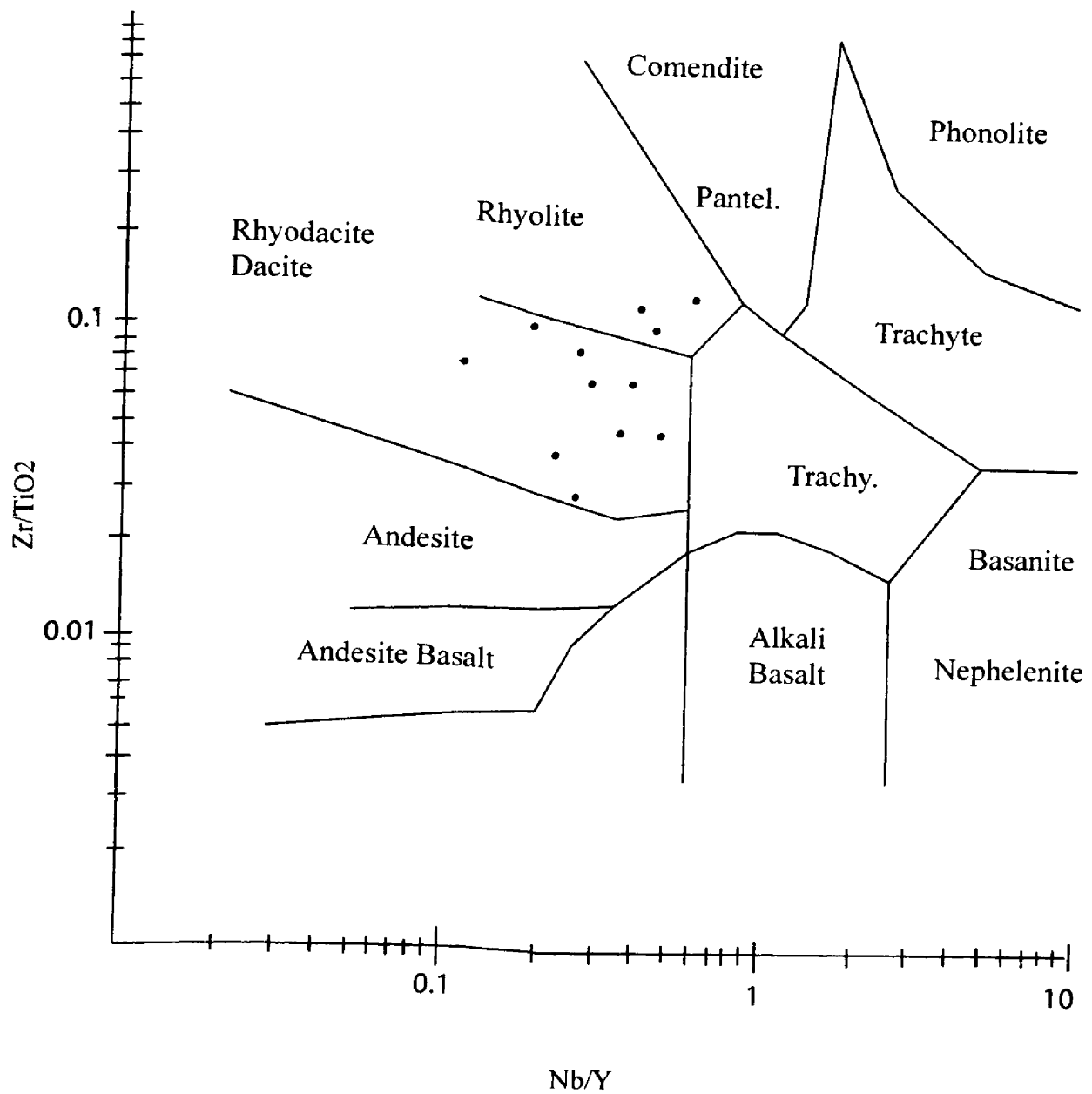


Figure 31: Plot of Zr/TiO₂ against Nb/Y following technique of Winchester and Floyd (1977). Belt K-bentonites plot in Rhyodacite/Dacite & Rhyolite areas.

Scanning-Electron Microscopy

SEM photographs reveal the fine-grained clay rich texture of the K-bentonite from the lower Garnet Range Formation. The larger platy mineral, which texturally resembles 2M1 illite or mica, shows surficial growth of clay, which resembles 1M illite, on the (001) surface.

Source of Illite and K-Bentonites in the Belt Supergroup

Illite is an abundant clay mineral throughout the geologic record, although weathering of crystalline rocks does not produce a significantly large amount of illite (Hoffman, 1979). However, large quantities of smectite form rapidly from devitrification of felsic volcanic ash. Data and interpretations presented in this paper suggest that the volumes of illite and chlorite in K-bentonites, argillites and siltites in the Belt Supergroup are a result of devitrification and subsequent diagenesis of air fall ash, as well as incorporation of terrigenous volcanic ash and detritus from an intracratonic source.

Source of Volcanic Ash in the Belt Basin

The volcanic ash in the Belt basin may have been derived from two source areas; from local sources as intracratonic rifting pulled the Belt basin apart and/or from the Southern Granite-Rhyolite complex and the Eastern Granite-Rhyolite complex to the southeast of the Belt basin that was active during Beltian time (Van Schmus and Bickford, 1993; Sears in review).

The Southern Granite-Rhyolite complex and the Eastern Granite-Rhyolite complex were active at about 1.4 to 1.34 Ga and 1.48-1.44 Ga, respectively (Van Schmus

and Bickford, 1993). This large complex extends from the buried Grenville front in eastern Ohio across the Texas panhandle and into northeastern New Mexico. The complex is predominately composed of rhyolite, dacite and shallow granitic plutons, with only a few sills of basalt and gabbro (Van Schmus and Bickford, 1993). Although much of the complex is not exposed, ring dike complexes associated with calderas may have been igneous centers that ejected felsic ash into the atmosphere. Sears (personal communication, 2005) suggests that the Southern Granite-Rhyolite complex, which was active during deposition of the Belt Supergroup may have supplied volumes of felsic volcanic ash to the Belt Basin.

Sears (in review) proposes a rifted-pediment model for the Belt basin, suggesting that the Belt basin initiated as a three-armed rift system that segmented a northwest sloping epi-continental pediment into a southern triangular wedge that received sediment from southwestern Laurentia, Siberia and northeastern Australia; and a northeastern triangular wedge that received sediment from the recycled pediment veneer and local bedrock (Figure 32). The recycled pediment veneer consists of felsic volcanic rocks and other sediments sourced from the Granite-Rhyolite complex located to the southeast of the Belt basin (Sears, in review). Because the Southern Granite-Rhyolite complex was explosively active during Beltian time, it is likely that air fall ash, along with volcanic and terrain sediment from the pediment veneer, was transported into the Belt basin supplying the large quantities of volcanic ash that may be the source of the volumes of illite and lesser amounts of chlorite in the Belt.

The single U-Pb zircon age of 1600 Ma from sample MF6031, the K-bentonite in the lower Garnet Range Formation (Missoula Group), (Chamberlain, personal

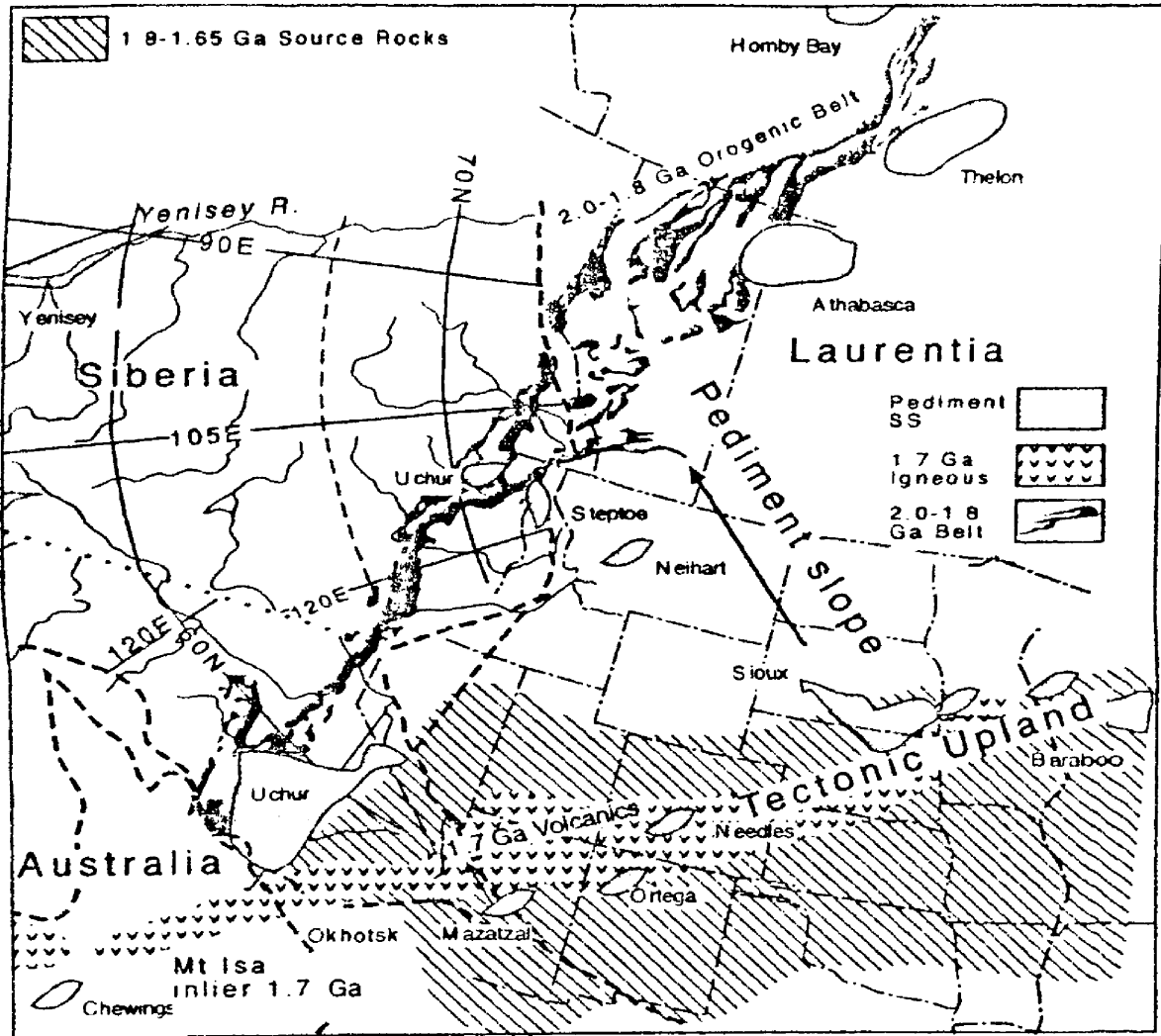


Figure 32: Proposed model of Sears (in review) showing the Tectonic Upland, Southern and Eastern Granite-Rhyolite Complex, to the southeast of the Belt basin that may have supplied volcanic ash to the Belt Supergroup.

communication, 2005) coincides with detrital zircon ages throughout the upper Belt. This age has been linked to the recycled pediment veneer described by Sears (in review). SHRIMP zircon ages from this K-bentonite may yield a non-detrital age corresponding to rhyolitic ash ejected during the eruptive phase of the Southern Granite-Rhyolite complex (Sears, in review). Goldich et al. (1959) dated a K-bentonite at Logan Pass in Glacier National Park at 1454 Ma and Evans et al. (2000) dated a K-bentonite at the Bonner-Libby contact at 1401 Ma. These ages are in agreement with the time frame in which the Southern Granite-Rhyolite complex was active and further supports the notion that the Granite-Rhyolite complex provided the volumes of volcanic ash to form the K-bentonites in the Belt Supergroup.

CHAPTER 6

CONCLUSIONS

1. Field characteristics, petrographic textural characteristics, mineral composition, polytype data, chemical compositions, and SEM characteristics collectively support the hypotheses that K-bentonites are abundant in the middle Proterozoic Belt Supergroup in western Montana and that explosive felsic volcanism was common during deposition of the Belt Supergroup.
2. Local explosive volcanism may have accompanied felsic and mafic activity as intracratonic rifting ripped the Belt basin apart.
3. The Southern Granite-Rhyolite complex and the Eastern Granite-Rhyolite complex active during Belt time may have been the sources of the numerous K-bentonites now recognized in the middle Proterozoic Belt Supergroup (Sears, in review).

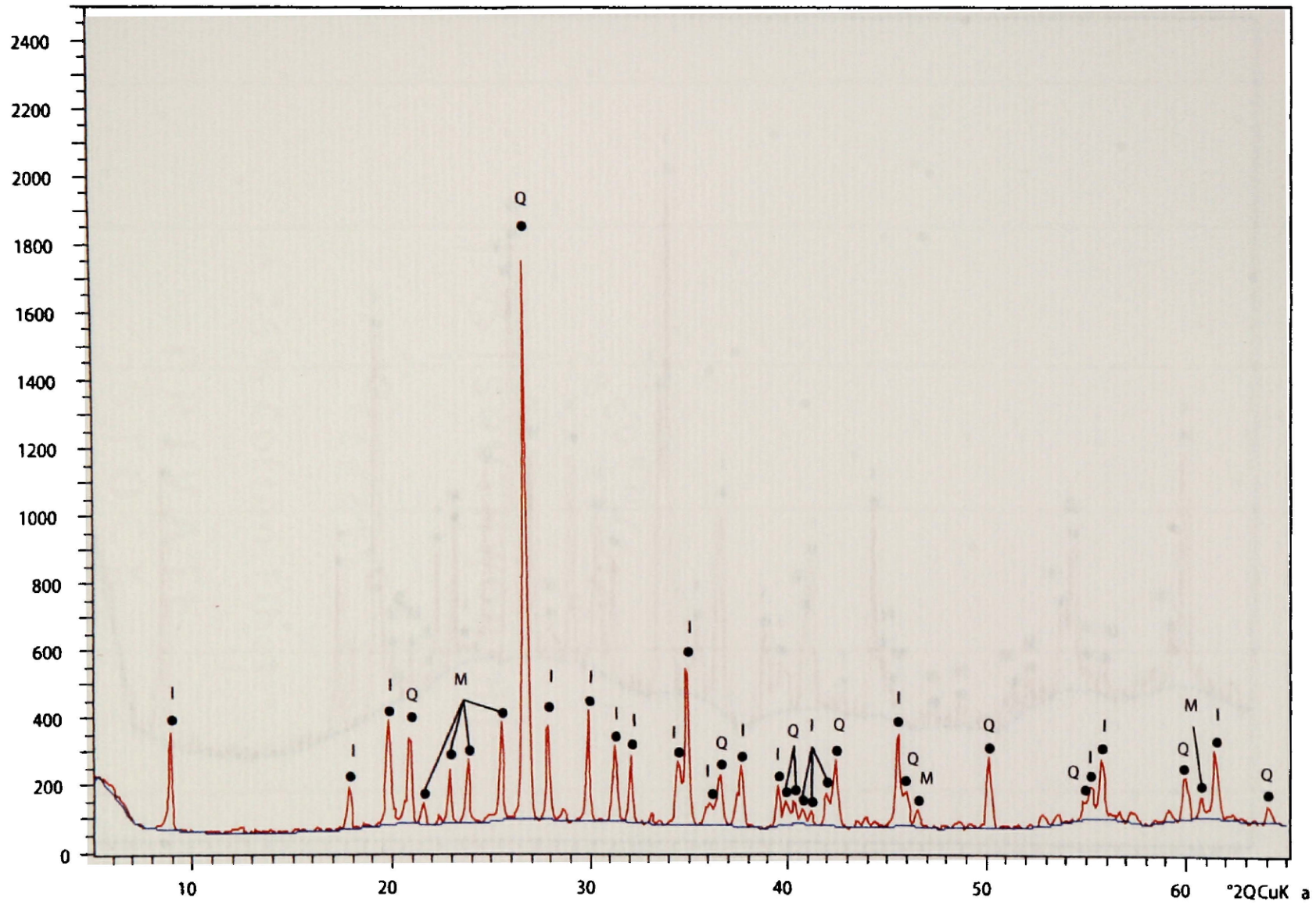
APPENDIX A
X-RAY DIFFRACTION PATTERNS

MF1031B

(K-Bentonite)

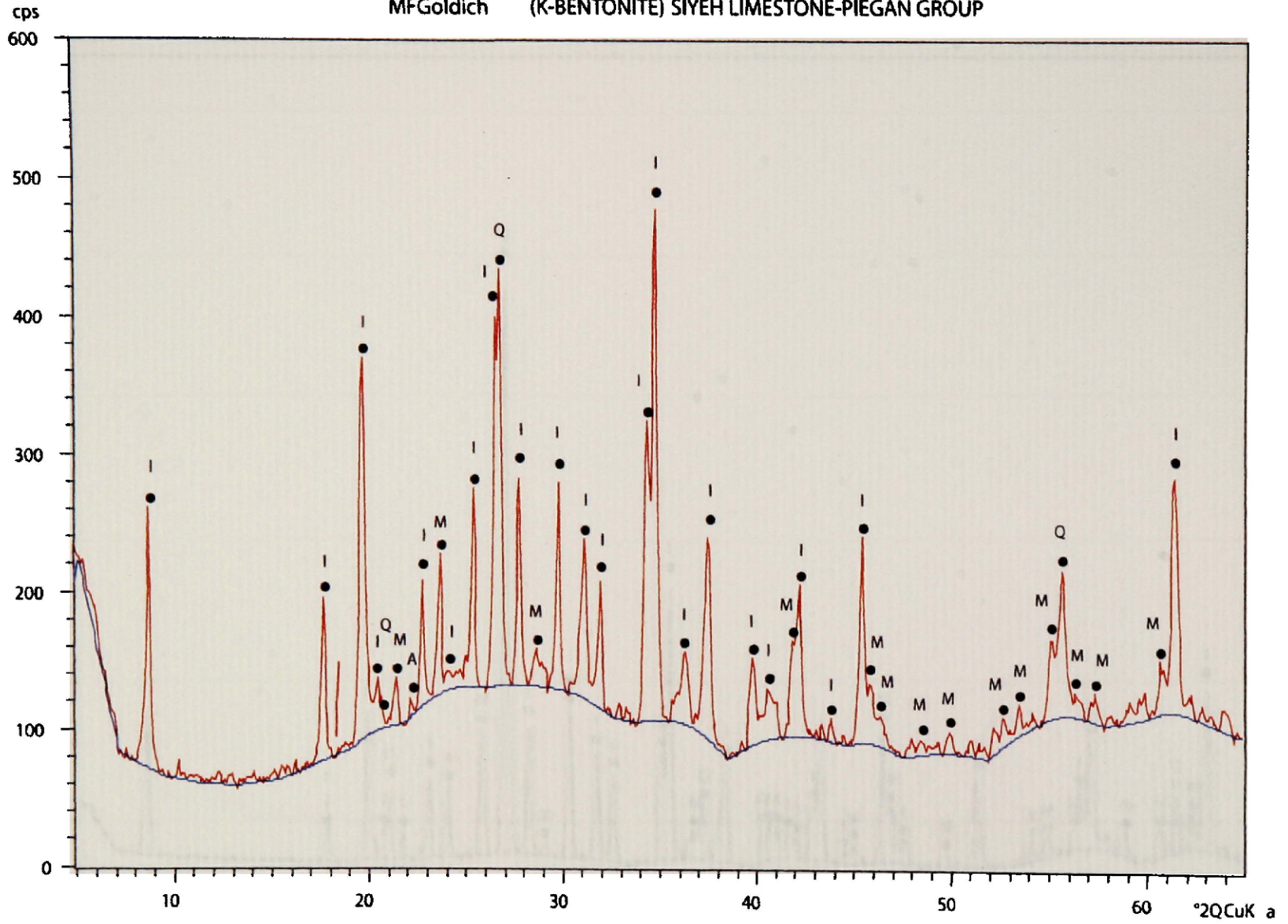
Revett Formation (Ravalli Group)

cps

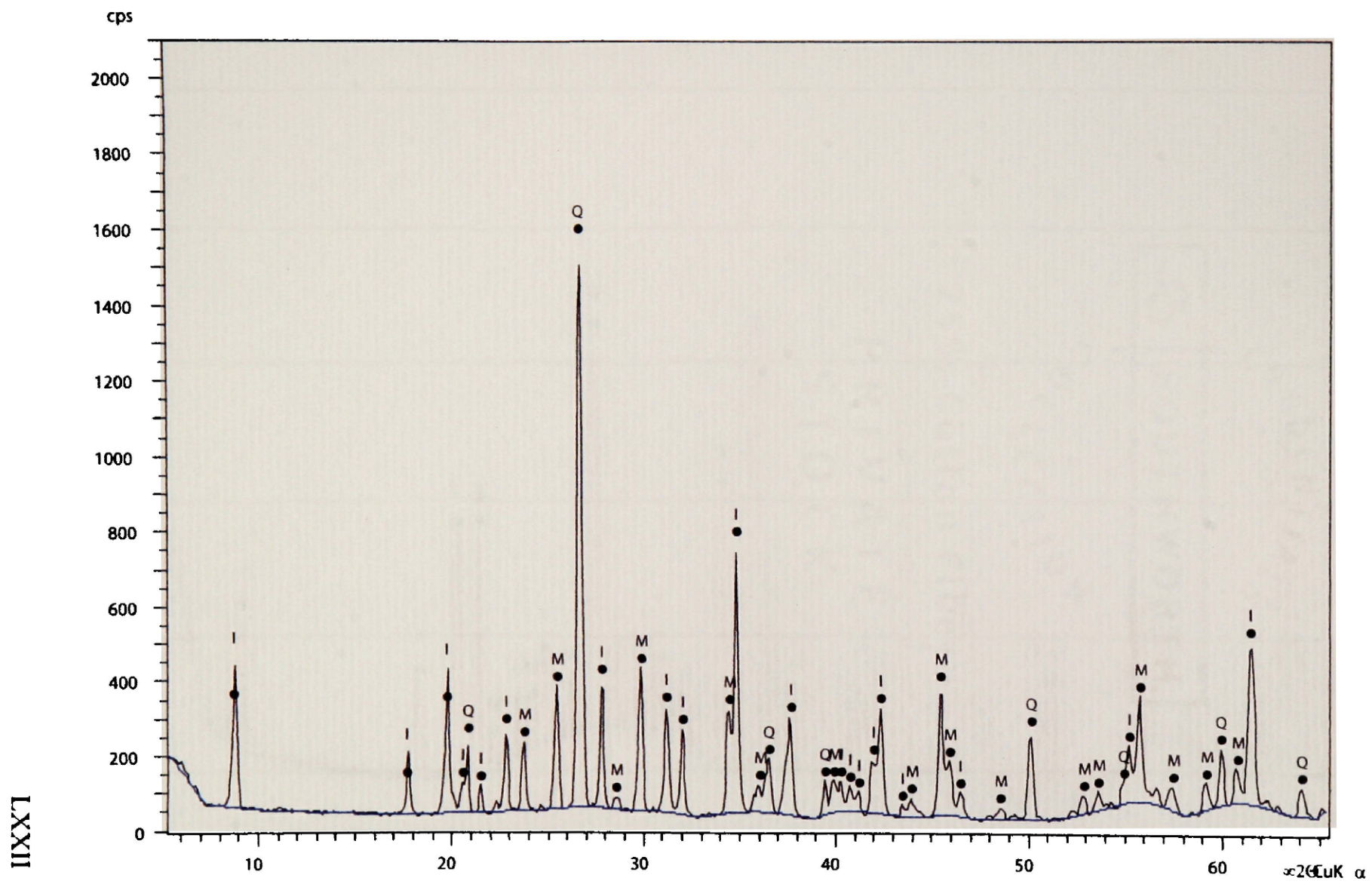


XX1

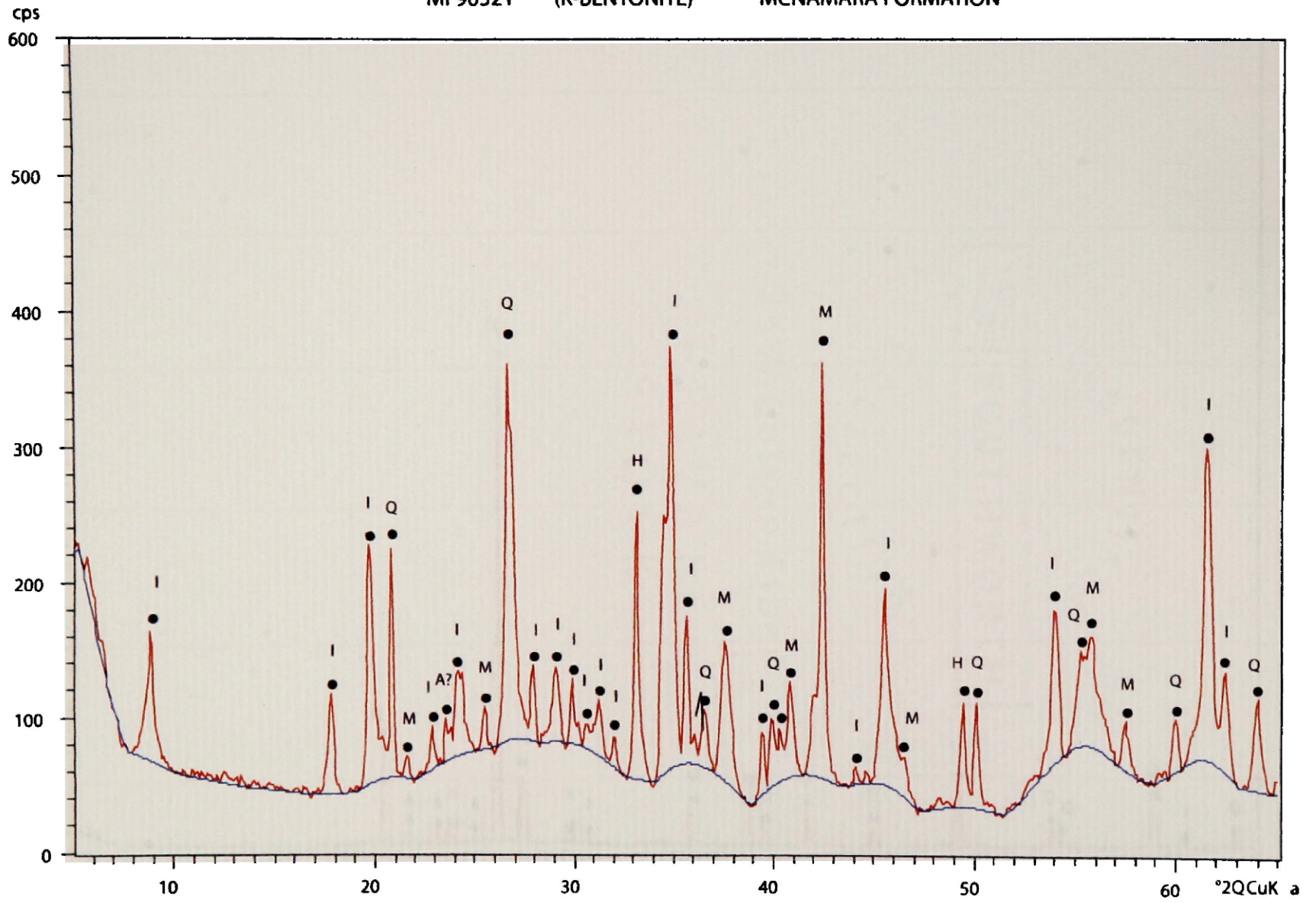
MFGoldich (K-BENTONITE) SIYEH Limestone-PIEGAN GROUP



MF19042 (K-bentonite) upper Bonner Formation

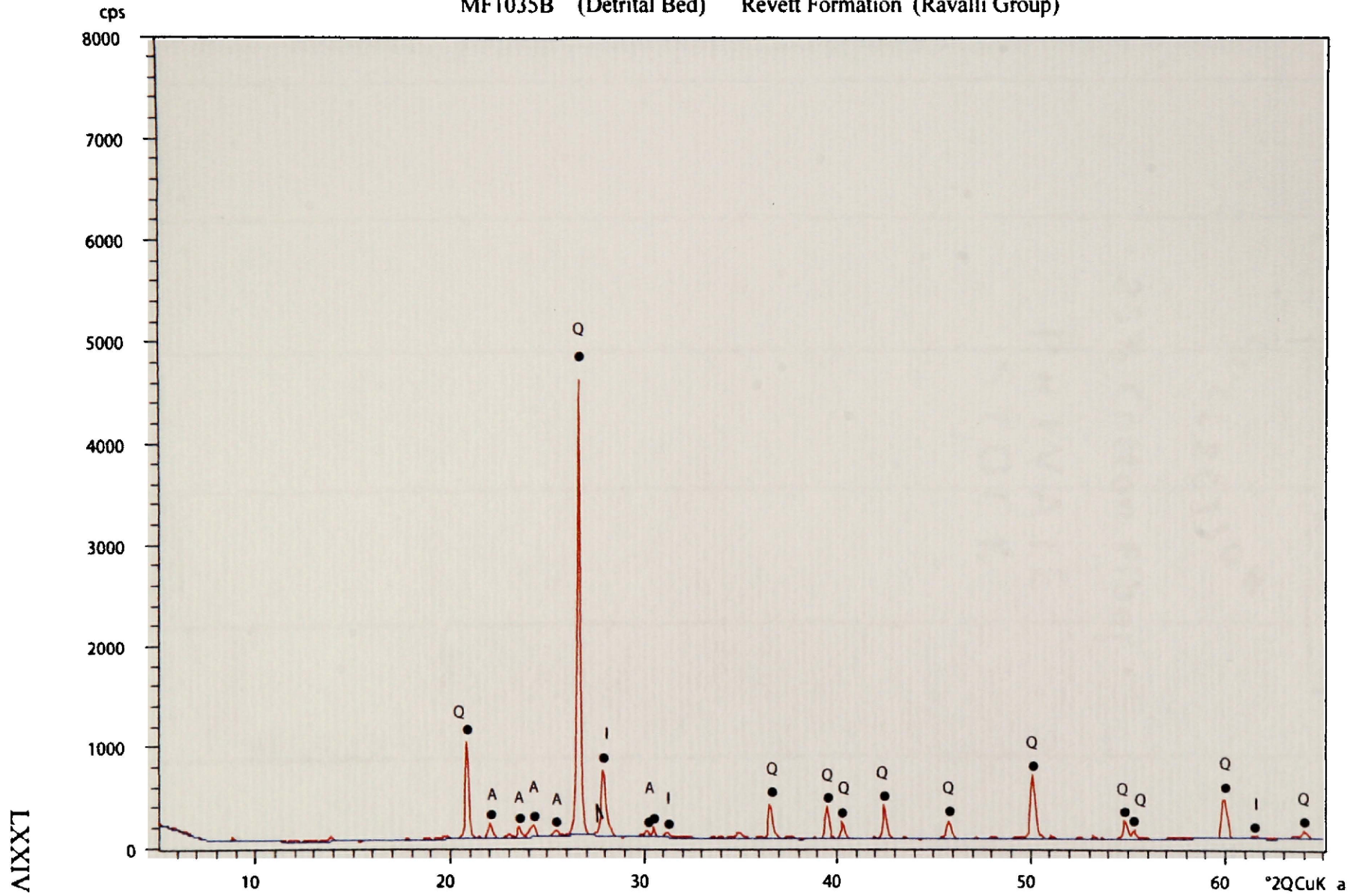


MF90321 (K-BENTONITE) MCNAMARA FORMATION



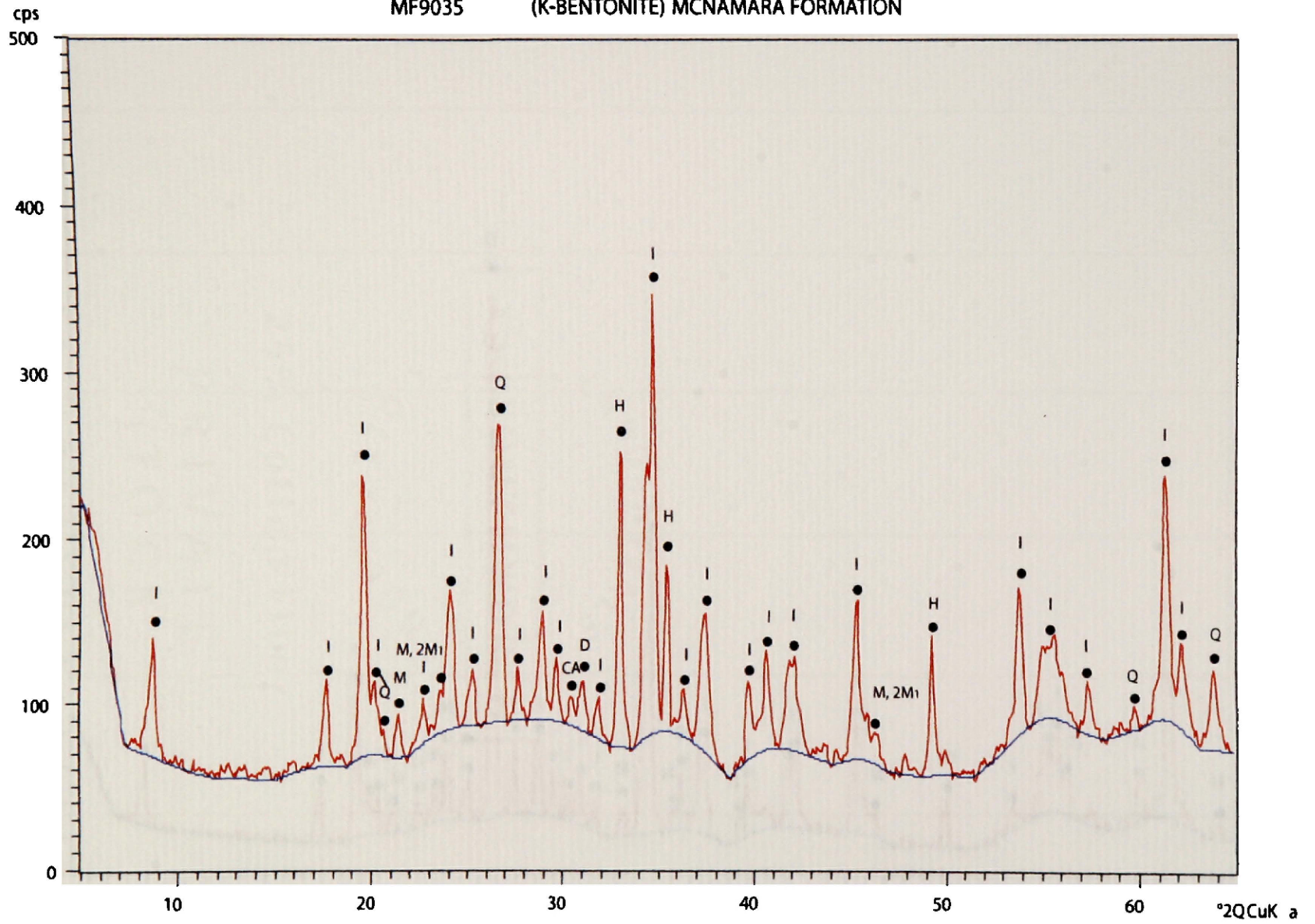
LXXXIII

MF1035B (Detrital Bed) Revett Formation (Ravalli Group)



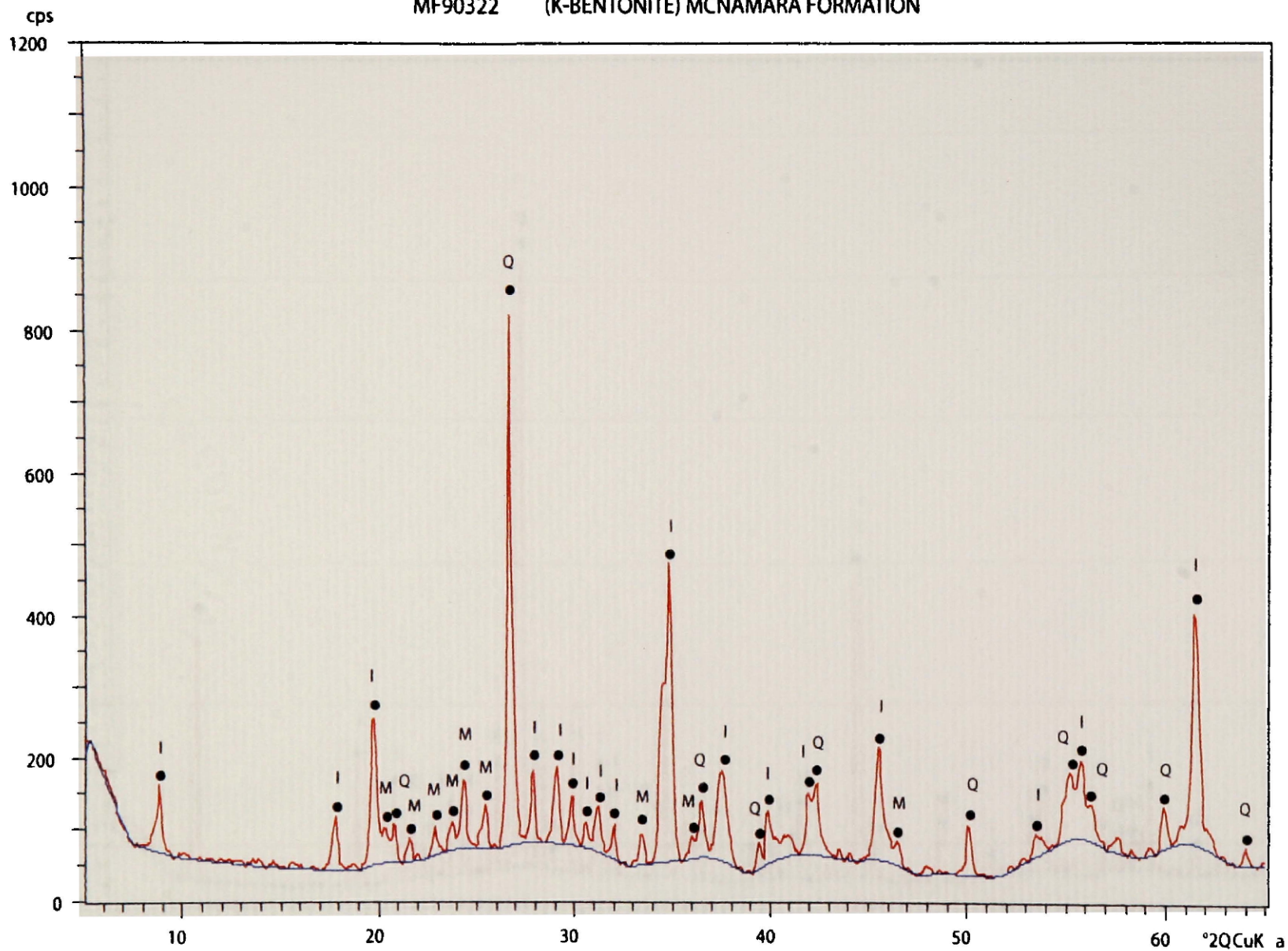
LXXIV

MF9035 (K-BENTONITE) MCNAMARA FORMATION



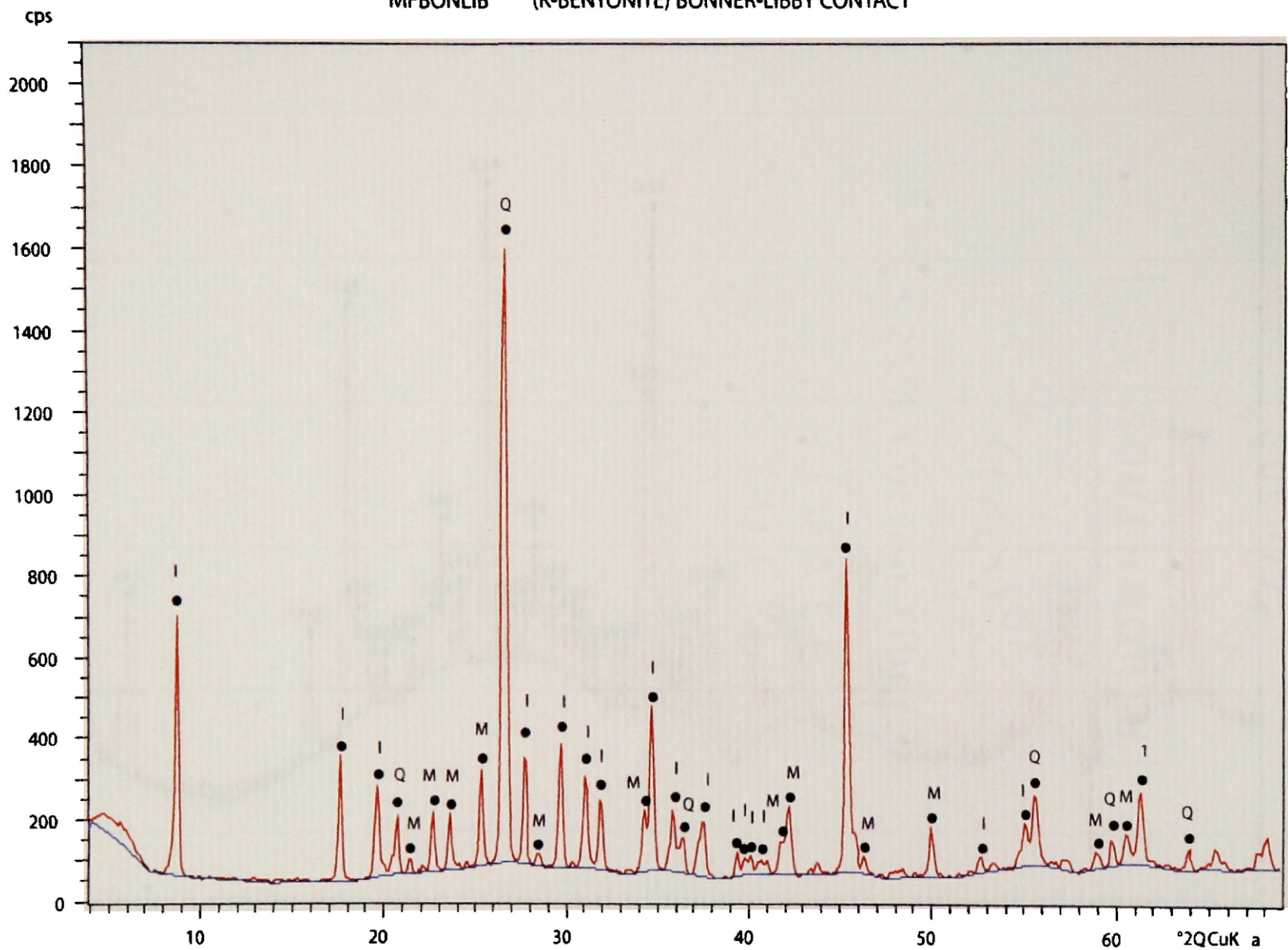
LXXV

MF90322 (K-BENTONITE) MCNAMARA FORMATION



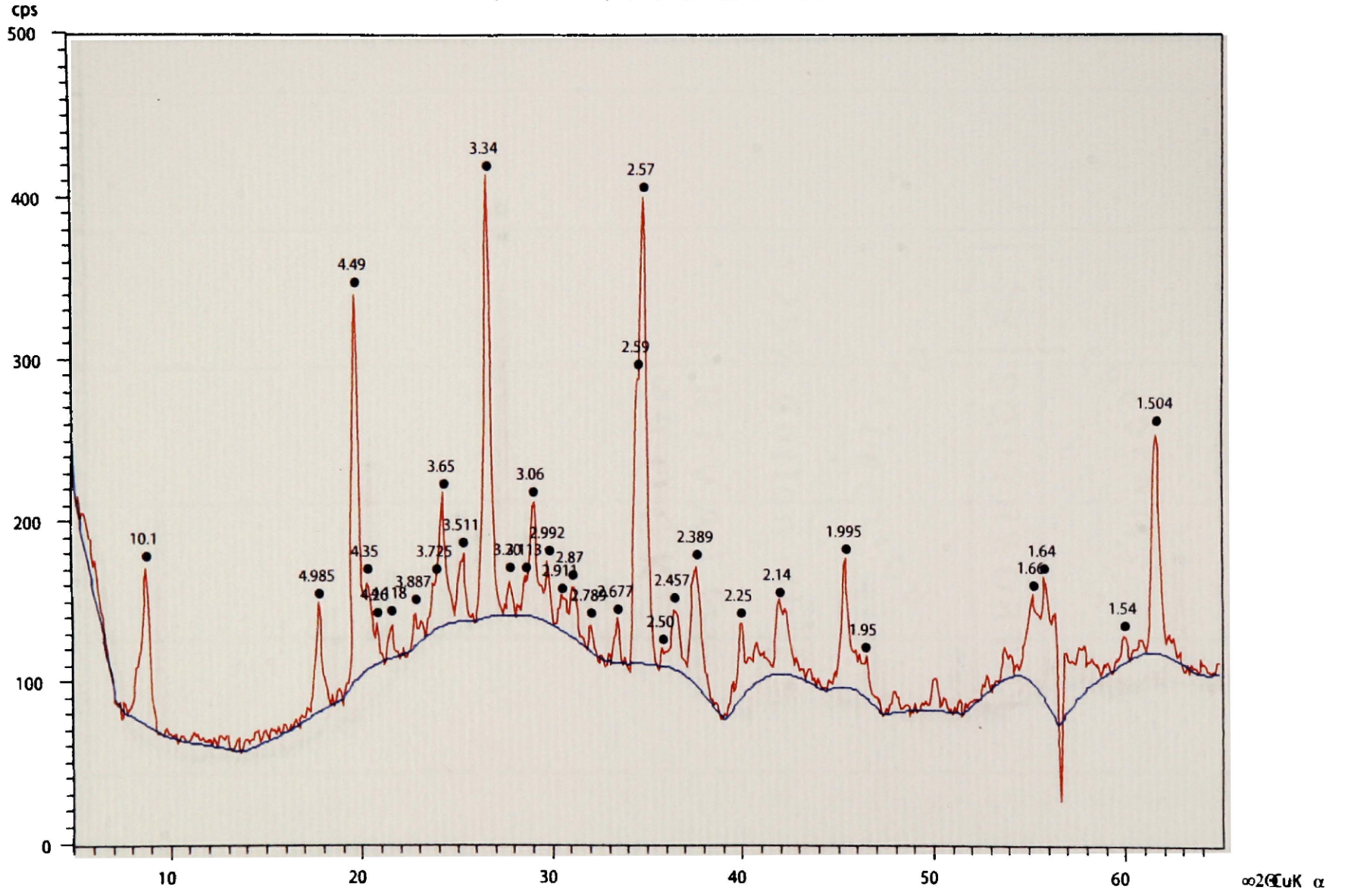
LXXVI

MFBNLIB (K-BENTONITE) BONNER-LIBBY CONTACT

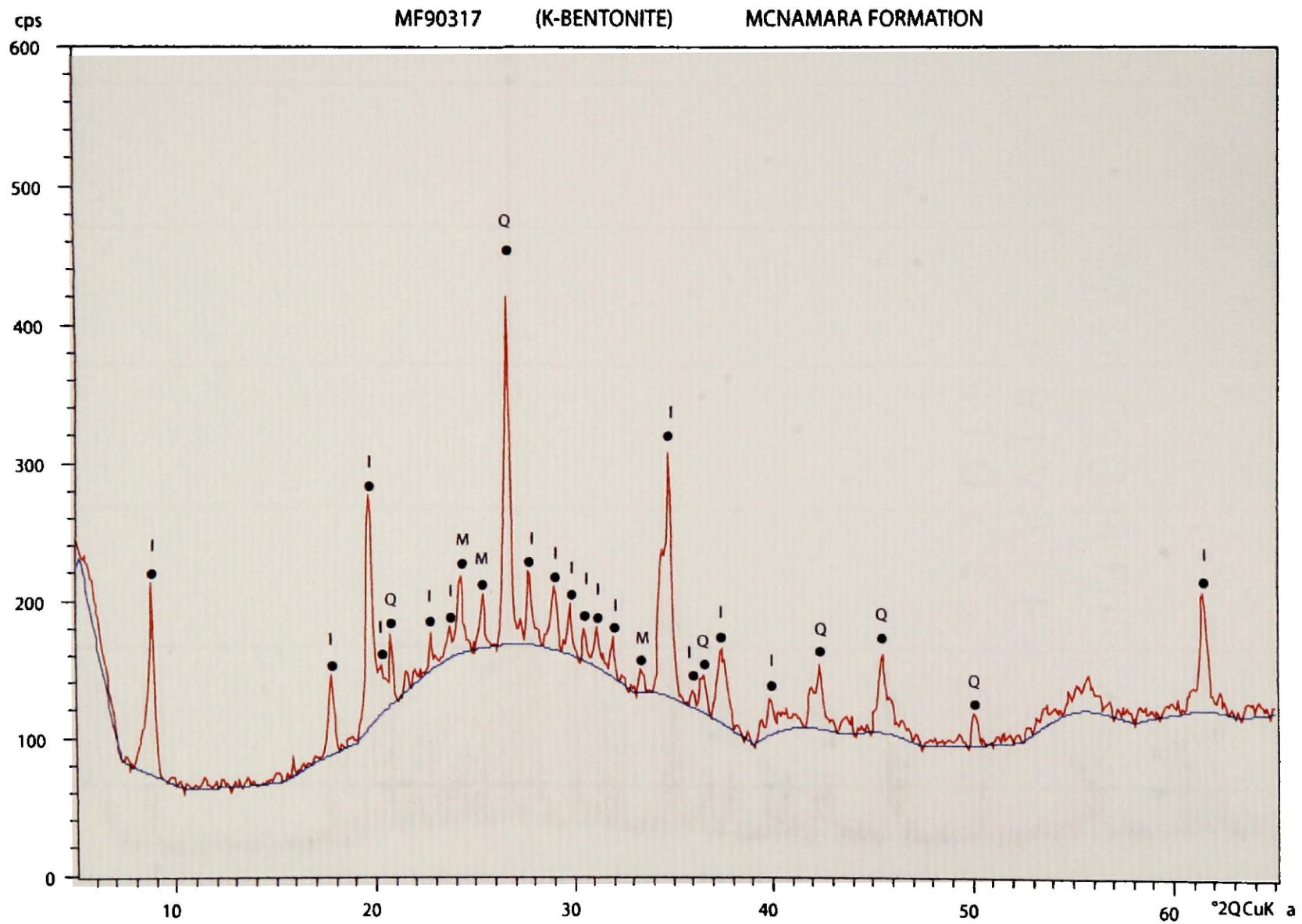


LXXVII

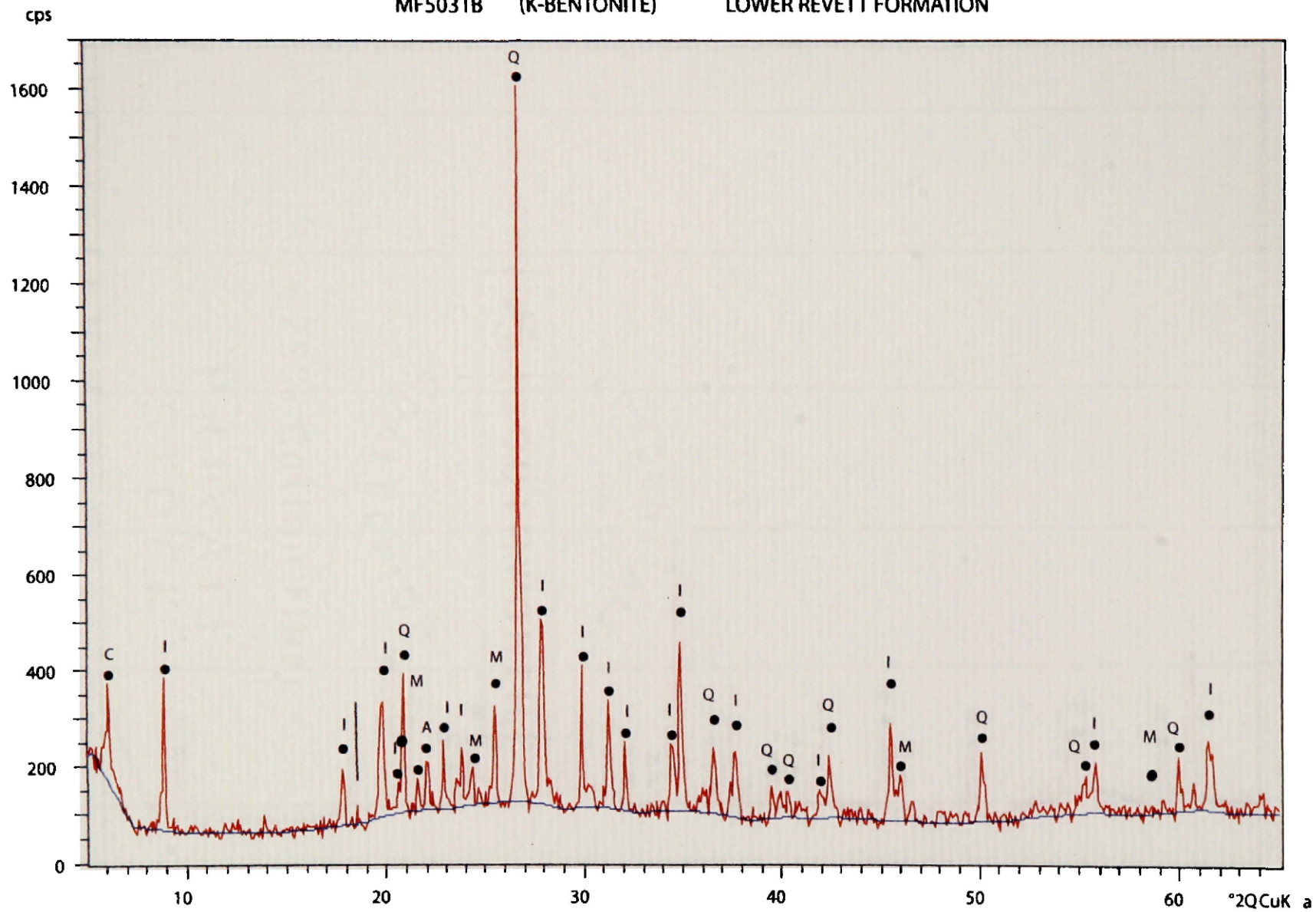
MF6031 (K-bentonite) lower Garnet Formation



LXXVIII

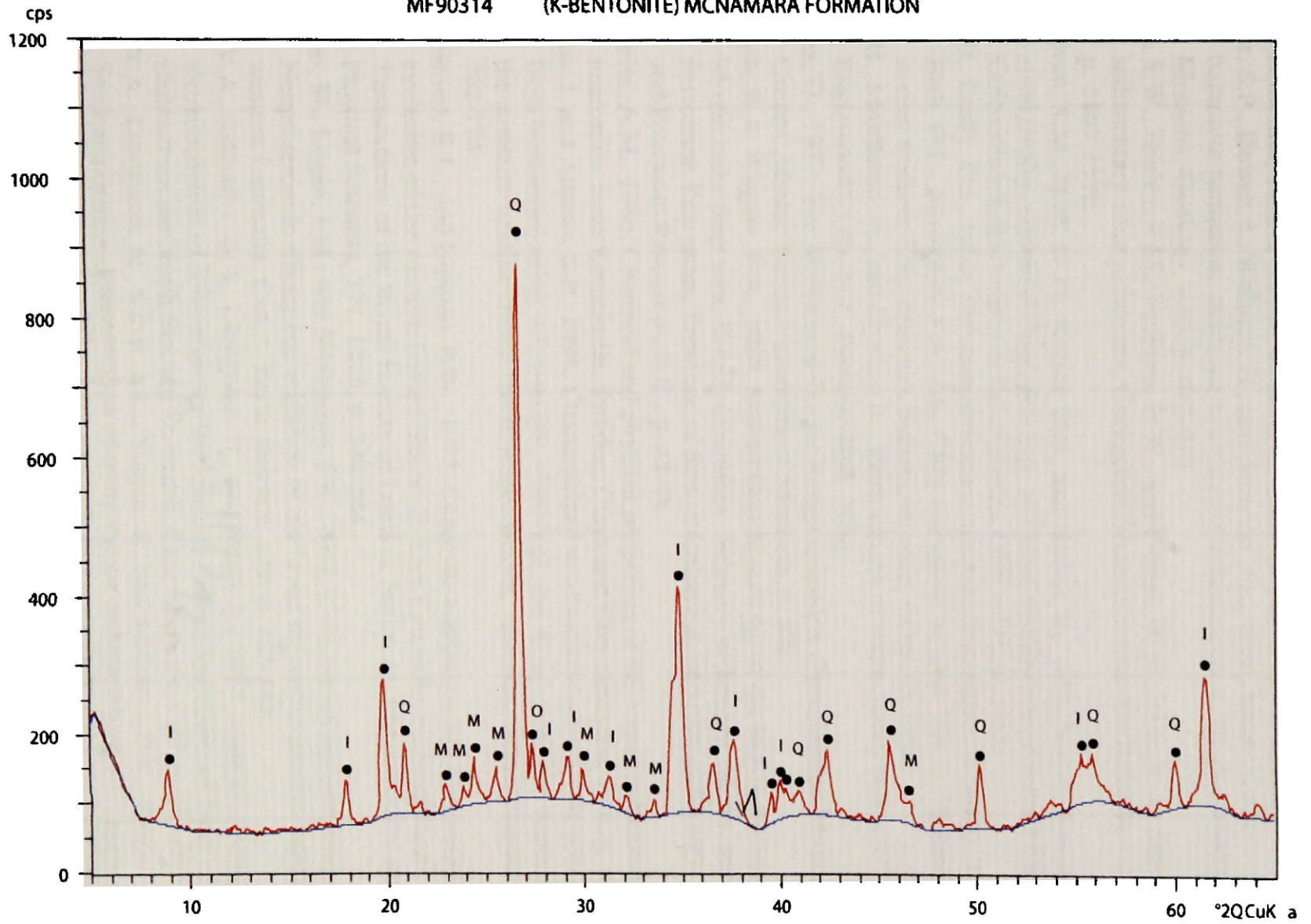


MF5031B (K-BENTONITE) LOWER REVETT FORMATION



XXXX

MF90314 (K-BENTONITE) MCNAMARA FORMATION



LXXXI

- Altaner, S., 1985, K+ metasomatism and diffusion in Cretaceous K-bentonites from the disturbed belt, northwestern Montana and in the Middle Devonian Tioga K-bentonite, eastern United States [PhD thesis]: University of Illinois.
- Altaner, S.P., Hower, J., Whitney, G., and Aronson, J.L., 1984, Model for K-bentonite formation: evidence from zoned K-bentonites in the disturbed belt, Montana: *Geology*, v.12, p. 412-415.
- Bailey, S.W., Hurley, P.M., Fairburn, H.W., and Pinson, W.H., 1962, K-Ar dating of sedimentary illite polytypes, *Geological Society of America Bulletin*, v.73, p. 1167-1170.
- Bergstrom, S.M., Huff, W.D., Kolata, D.R., and Heikki, B., 1995, Nomenclature, stratigraphy, chemical fingerprinting, and areal distribution of some Middle Ordovician K-bentonites in Baltoscandia, *GFF*, v117, p. 1-13.
- Bish, D., Duffy, C.J., 1990, Thermogravimetric analysis of minerals in Stucki, J.W., Bish, D.L., Mumpton, F.A., eds. CMS workshop lectures Vol. 3, Thermal analysis in clay science, Clay Minerals Society, Boulder CO p. 95-189.
- Blatt, H., Middleton, G., and Murray, R., 1980, Origin of sedimentary rocks, 2nd edition: Englewood Cliffs, N.J., Prentice-Hall, 766p.
- Bleiwas, D., 1977, The McNamara-Garnet Range transition (Precambrian Missoula Group), Master Thesis University of Montana, p. XX.
- Burwash, R.A. Wagner, P.A., 1988, Sm/Nd Geochronology of the Moyie intrusions, Moyie Lake map area, British Columbia. Ministry of Energy, Mines, and Petroleum Resources, Province of British Columbia, Ministry of Energy, Mines, and Petroleum Resources, B.C., p. 45-48.
- Brusewitz, A.M., 1986, Chemical and physical properties of Paleozoic potassium bentonites from Kinnekulle, Sweden, *Clays and Clay Minerals*, v.34, p. 442-454.
- Cuadros, J. and Altaner, S.P., 1998, Characterization of mixed-layered illite-smectite from bentonites using microscopic, chemical, and X-ray methods: constraints on the smectite-to-illite transformation mechanism, *American Mineralogist*, v.83, p. 762-774.
- Christiansen, R.L., and Lipman, P.W., 1972, Cenozoic volcanism and plate-tectonic evolution of the western United States; II, Late Cenozoic, *Philosophical Transactions of the Royal Society of London, Series A: Mathematical and Physical Sciences*, 271, 1213, p. 249-284.
- Colpron, M., Logan, J.M., and Mortensen, J.K., 2002, U-Pb zircon age constraint for late Neoproterozoic rifting and initiation of the lower Paleozoic passive margin of western Laurentia, *Can. J. Earth. Science*, v39, p. 133-143.
- Drits, V.A., Sakbarov, B.A., Lindgreen, H., and Salyn, A., 1997, Sequential structure transformation of illite-smectite-vermiculite during diagenesis of Upper Jurassic shales from the North Sea and Denmark, *Clay Minerals*, v.32, p. 351-371.
- Drits, V.A., Lindgreen, H., Salyn, A.L., Ylagan, R., and McCarty, D.K., 1998, Semiquantitative determination of trans-vacant and cis-vacant 2:1 layers in illites and illite-smectites by thermal analysis and X-ray diffraction, *Am. Mineralogist*, V83, p1188-1198.
- Eberl, D.D., and Hower, J (1976) Kinetics of illite formation. *Geol. Soc. Am Bull.*, v87, 1326-1330.

- Elliott, W.C., and Aronson, J., L., 1987, Alleghanian episode of K-bentonite illitization in the southern Appalachian Basin, *Geology* V15, 735-739
- Eslinger, E., and Sellars, B., 1981, Evidence for the formation of illite from smectite during burial metamorphism in the Belt Supergroup, Clark Fork, Idaho, *J. of Sed. Pet.*, v51, n1, p. 203-216.
- Evans, K.V., Aleinikoff, J.N., Obradovich, J.D., and Fanning, C.M., 2000, *Can. J. Earth. Science*, v37, p. 1287-1300.
- Evans, K.V., and Fischer, L.B., 1986, U-Pb geochronology of two augen gneiss terranes, Idaho; new data and tectonic implications, *Canadian Journal of Earth Science*, v.23, n.12, p. 1919-1927.
- Frost, C.D., and Winston, D., 1984, Nd isotope systematics of coars- and fine-grained sediments; examples from the middle Proterozoic Belt-Purcell Supergroup, *Journal of Geology*, v.95, n.3, p.309-327.
- Goldich, S.S., Baadsgaard, H., Edwards, G., and Weaver, C.E., 1959, Investigations in radioactivity dating of sediments: *American Association of Petroleum Geologists Bulletin*, v.43 p. 654-662.
- Grim, R.E., and Guven, N., 1978, *Bentonites: geology, mineralogy, properties and uses*, Elsevier Scientific Publishing Company, NY.
- Gruner, J.W., 1940, Cristobalite in bentonite, *Am. Mineralogist*, v.25, 587-590, in Slaughter, M. & Earley, J.W., 1965, *Mineralogy and geological significance of the Mowry bentonites, Wyoming. Geol. Soc. Am. Spec. Paper 83*
- Harrison, JE, 1972, Precambrian belt basin of the northwestern United States, its geometry, sedimentation, and copper occurrences: *Geological society of america bulletin*, v83, p1215-1240.
- Haynes, J.T., 1994, The Ordovician Deicke and Millbrig K-bentonite beds of the Cincinnati Arch and the Southern Valley and Ridge Province, *Geological society of america special paper 290*. 80p.
- Hoffman, J., and Hower, J., 1979, Clay mineral assemblages as low grade metamorphic geothermometers; application to the thrust faulted disturbed belt of Montana, U.S.A., In Scholle, P.A., and Schluger, P.R. (eds), *Aspects of diagenesis, SEPM spec. pub.*, Society of Economic Paleontologists and Mineralogists, v. 26, p. 55-79.
- Hoffmann, J., 1976. Regional metamorphism and K-Ar dating of clay minerals in Cretaceous sediments of the disturbed belt of Montana, Ph.D. dissertation, Case Western Reserve University, Cleveland.
- Hower, J., Eslinger, E.V., Hower, M., and Perry, E.A., 1976, The mechanism of burial metamorphism of argillaceous sediments: 1. Mineralogical and chemical evidence: *Geological Society of America Bulletin*, v.87, p. 725-737.
- Huff, W.D., Bergstrom, S.M., Kolata, D.R., and Sun, H., (1997), The Lower Silurian Osmondburg K-bentonite Part II: mineralogy, geochemistry, chemostratigraphy and tectonomagmatic significance. *Geol. Mag.* V135, 15-26.
- Hyndman, D (1985) *Petrology of igneous and metamorphic rocks* 2nd edition, McGraw-Hill, Inc.
- Jackson, M.L., 1958, *Soil chemical analysis*, Prentice-Hall, Englewood Cliffs, N.J.

- Kiersch, G.A. and Keller, W.D., 1955, Bleaching clay deposits, Defiance Plateau District, Arizona, *Econ. Geol.* V50, 469-494, in Altaner, S.P., 1989, Calculation of K diffusional rates in bentonite beds, *Geochemica et Cosmochimica Acta*, v53, 923-931.
- Kidder, D.L., 1992, Stratigraphy and sedimentology of the Libby Formation, Belt Supergroup (Middle Proterozoic) of Montana and Idaho, U.S.A. *Contributions to Geology*, University of Wyoming, 29:119-131; in Evans, K.V., Aleinikoff, J.N., Obradovich, J.D., and Fanning, C.M., 2000, SHRIMP U-Pb geochronology of volcanic rocks, Belt Supergroup, western Montana: evidence for rapid deposition of sedimentary strata, *Can. J. Earth Sci.* V37, 1287-1300
- Kolata, D.R., Huff, W.D., and Bergstrom, S.M., 1996, Ordovician K-bentonites of Eastern North America: Special Paper 313 Geological Society of America, 84p.
- Lydon, J.W., 2000, A synopsis of the current understanding of the geological environment of the ullivan deposit, chapter 3 in Lydon, JW, Hoy, T, Slack, JF, and Knapp, ME eds, the geological environment of the sullivan deposit, B.C.: Geological association of canada, mineral deposits division special pub no. 1, p 12-31.
- Link, P.K., Winston, D., and Boyack, D, Stratigraphy of the Mesoproterozoic Belt Supergroup, Salmon River Mountains, Lemhi County, Idaho, In Lageson, D.R., Christner, R.B. (eds), 2003 Tobacco Root Geological Society field conference at the Belt symposium IV, *Northwest Geology*, v. 32 p. 107-123.
- McCarty, D., 1990, Burial diagenesis in two non-marine Tertiary basins, southwestern Montana, M.S., University of Montana.
- 2002, Quantitative mineral analysis of clay-bearing mixtures: “The Reynolds Cup” Contest. *IUCr CPD Newsletter*, 27, p. 12-16, <http://www.iucr.org/iucr-top/comm/cdp/html.newsletter27.html>.
- Moe, J.A., Ryan, P.C., Elliott, W.C., and Reynolds, R.C., 1996, Petrology, chemistry, and clay mineralogy of a K-Bentonite in the Proterozoic Belt Supergroup of western Montana: *Journal of Sedimentary Research*, v.66, p. 95-99.
- Moore, D., and Reynolds, R.C., 1997, X-ray diffraction and the analysis of clay minerals, 2nd edition, Oxford University Press, Oxford, UK, 378 p.
- Moyer, T.C., and Nealey, L.D., 1989, Regional compositional variations of late Tertiary bimodal rhyolite lavas across the Basin and Range/ Colorado Plateau boundary in western Arizona, In Leeman, W.P., and Fitton, J.G., (eds), Special section on magmatism associated with lithospheric extension, *Journal of Geophysical Research*, B, Solid Earth Planets, v.96, n.6, p. 7799-7816.
- Mundil, R., Brack, P., Meier, M., Rieber, H., and Oberli, F., 1996, High resolution U-Pb dating of Middle Triassic volcanoclastics ; time-scale calibration and verification of tuning parameters for carbonate sedimentation, *Earth and Planetary Science Letters*, v. 141 n.1-4, p. 137-151.
- Nanson, G.C., Rust, B.R., and Taylor, G., 1986, Coexistent mud braids and anastomosing channels in an arid-zone river: Cooper Creek, central Australia, *Geology*, v.14, n.2, p. 175-178.

- Pallister, J.S., 1987, Magmatic history of Red Sea rifting; perspective from the central Saudi Arabian coastal plain; with Suppl. Data 87-11, Geological Society of America Bulletin, v.96, n.4, p. 400-417.
- Perry, E., and Hower, J., 1972, Late-stage dehydration in deeply buried polytropic sediments: American Association of Petroleum Geologists Bulletin, v. 56, p. 2013-2021.
- Ray, J.S., Martin, M.W., Veizer, J., and Bowring, S.A., 2002, U-Pb zircon dating and Sr isotope systematics of the Vindhyan Supergroup, India, Geology, v.30, n.2, p. 131-134.
- Reinink-Smith, L.M., 1990, Mineral assemblages of volcanic and detrital partings in Tertiary coal beds, Kenai Peninsula, Alaska, Clays and Clay Minerals, V38, n1, 97-108.
- Rosenkrans, R.R., 1936, Stratigraphy of the Ordovician bentonite beds in southwestern Virginia: Va. Geol. Survey Bull., v46, 85-111 in Slaughter, M. & Earley, J.W., 1965, Mineralogy and geological significance of the Mowry bentonites, Wyoming. Geol. Soc. Am. Spec. Paper 83
- Ross, G.M., Villeneuve, M., 2003, Provenance of the Mesoproterozoic (1.5 Ga) Belt basin (western North America): Another piece in the pre-Rodinia paleogeographic puzzle, GSA Bulletin, V115, n10, p1191-1217.
- Ross, C.S., 1928, Altered Paleozoic volcanic materials and their recognition, Bull. AAPG V12, p. 143-164.
- Ryan, P., 1991, Structural variations in illite and chlorite in the Belt Supergroup, western Montana and northern Idaho [Masters thesis]: Missoula, Montana, University of Montana, 48p.
- Schieber, J., 1993, Survey of sedimentologic, geochemical and mineralogical features of the Belt Series and their bearing on the lacustrine vs. marine debate; in Belt Symposium III, Informal Program and Abstracts: Whitefish, Montana, 3 p.
- Schirnack, C., 1990, Origin, sedimentary geochemistry, and correlation of Middle and Late Ordovician K-bentonites: constraints from melt inclusions and zircon morphology, [unpublished Master's thesis]: Albany, New York, State University of New York, 209pp.
- Sears, J.W., in review, Destabilization of a Proterozoic epi-continental pediment by rifting: a model for the Belt-Purcell Basin, North America.
- Sears, J., 2005, Destabilization of a Proterozoic epi-continental pediment by rifting: a model for the Belt-Purcell Basin North America, In review.
- Saylor, B.Z., Poling, J.M., and Huff, W., In Review, Stratigraphic and geochemical correlation of ash beds in the terminal Proterozoic Nama Group, Geological Magazine.
- Slaughter, M. & Earley, J.W., 1965, Mineralogy and geological significance of the Mowry bentonites, Wyoming, Geol. Soc. Am. Spec. Paper 83
- Srodon, J. and Eberl, D.D. (1984) Illite, In Bailey, SW (Ed) Reviews in Mineralogy Vol 13 Micas, Mineralogical Society of America, chp. 12, p 495-544.
- Srodon, J., Drits, V.A., McCarty, D.K., Hsieh, J.C.C., and Eberl, D., 2001, Quantitative x-ray diffraction analysis of clay-bearing rocks from random preparations, Clays and Clay Minerals V49 n6

- Tucker, R.D., and McKerrow, W.S., 1995, Early Paleozoic chronology; a review in light of new U-Pb zircon ages from Newfoundland and Britain, *Canadian Journal of Earth Sciences*, v. 32 n.4, p. 368-379.
- Van Schmus, W.R., and Bickford, M.E., 1993, Transcontinental Proterozoic provinces, in Reed, J.C., et al., eds., *Precambrian: Continental U.S.: Boulder, Colorado, Geological Society of America, Geology of North America*, v. C-2, p. 171-334.
- Velde, B., and Brusewitz, A.M., 1982, Metasomatic and nonmetasomatic low-grade metamorphism of Ordovician metabentonites in Sweden, *Geochem Cosmochim Acta*, V46, p. 447-452.
- Walker, S.C., 1983, The nature and origin of bentonites and potassium bentonites, northwestern Montana [Masters thesis]: Missoula, Montana, University of Montana, 33p.
- Walker and Thompson, 1990, Structural variations in chlorite and illite in a diagenetic sequence from the Imperial Valley, California, *Clays and Clay Minerals*, v. 38, p. 315-321.
- Weaver, C.E., 1953, Mineralogy and petrology of some ordovician k-bentonites and related limestones., *Bulletin of the geological society of america.*, V64 p921-944.
- Wearver, C.E., and Wampler, J.M., 1970, K, Ar, illite burial: *Geological Society of America Bulletin*, v. 81, p. 3423-3430.
- Winchester, J.A., and Floyd, P.A., 1977, Geochemical discrimination of different magma series and their differentiation products using immobile elements, *Chemical Geology*, v. 20, p. 325-343.
- Winston, D., 1986, Sedimentology of the Ravalli Group, middle Belt carbonate and Missoula Group, middle Proterozoic Belt Supergroup, Montana, Idaho and Washington, In Roberts, S.M. (ed) *Belt Supergroup, a guide to Proterozoic rocks of western Montana and adjacent areas, Special Publication-State of Montana Bureau of Mines and Geology*, 94, p. 85-124.
- Winston, D., 1986, Stratigraphic correlation and nonmenclature of the middle Proterozoic Belt Supergroup Montana, Idaho, and Washington, In Roberts, S.M., (ed.), *Belt Supergroup, Montana Bureau of Mines and Geology, special paper 94*, p.69-84.
- Winston, D., (2003) Proposed revisions of the Helena and Wallace Formations, Mid Proterozoic Belt Supergroup, Montana and Idaho, *Northwest Geology*, in Lageson, D.R. et al. (eds), 2003 Tobacco Root Geological Society field conference at the Belt Symposium IV, V32, p. 172-178.
- Yoder, H.S., and Eugster, H.P., 1955, Synthetic and natural muscovites, *Geochimica et Cosmochimica Acta*, v.8, n.5-6, p. 225-280.
- Zartman, R.E., Peterman, Z.E., Obradovich, J.D., Gallego, M.D., Bishop, D.T., 1982, Age of the Crossport C sill near Eastport, Idaho, *Special publication, State of Montana Bureau of Mines and Geology*, 90, Montana Bureau of Mines and Geology, Butte p 82-84.